Design of an indirect-fired falling-particle air preheater for MHD power generation
by Chris Dewey Jensen

A thesis submitted in partial fulfillment of the requirements for the degree of MASTER OF SCIENCE in Chemical Engineering
Montana State University

Abstract:
A preliminary design for an indirect-fired falling-particle air preheater for a 400 MW (thermal) MHD power generation plant was made.

The project was broken down into three major parts: material properties prediction, development of a theoretical model, and capital and annual cost estimation of the overall design.

A theoretical model was developed for an indirect-fired cored-brick air preheater. Capital and annual costs were estimated and compared to those of the falling-particle air preheater. It was found that overall air preheat systems involving these two designs would have approximately the same capital costs of ~ $44 x 10^6, and annual costs of ~$6 x 10^6.

An economic comparison was then made between overall indirect-fired air preheat designs, and overall direct-fired designs. In both the falling-particle and cored-brick cases, the capital cost of the indirect-fired design was approximately 50% greater than the capital cost of the direct-fired design.

STATEMENT OF PERMISSION TO COPY

In presenting this thesis in partial fulfillment of the requirements for an advanced degree at Montana State University, I agree that the Library shall make it freely available for inspection. I further agree that permission for extensive copying of this thesis for scholarly purposes may be granted by my major professor, or, in his absence, by the Director of Libraries. It is understood that any copying or publication of this thesis for financial gain shall not be allowed without my written permission.

Signature Chris Dewey Jensen

Date June 21, 1976

DESIGN OF AN INDIRECT-FIRED FALLING-PARTICLE AIR PREHEATER FOR MHD POWER GENERATION

by

CHRIS DEWEY JENSEN

A thesis submitted in partial fulfillment
of the requirements for the degree

of

MASTER OF SCIENCE

in

Chemical Engineering

Approved:

William Lenth
Chairperson, Graduate Committee

Lloyd Berg
Head, Major Department

Henry L Parsons
Graduate Dean

MONTANA STATE UNIVERSITY
Bozeman, Montana

August, 1976

ACKNOWLEDGMENT

The author wishes to give special thanks to Dr. William Genetti for his invaluable support in the development of this project.

Special thanks also goes to Dr. R. L. Mussulman of the Mechanical Engineering Department of his many helpful suggestions.

The author gratefully acknowledges financial support from ERDA/MHD Division.

Finally, thanks goes to Sherry Greene, secretary for the Chemical Engineering Department, for her typing of this thesis.

TABLE OF CONTENTS

	Page
VITA	ii
ACKNOLWEDGMENTS	iii
LIST OF TABLES	viii
LIST OF FIGURES	ix
NOMENCLATURE	x
ABSTRACT	xii
INTRODUCTION	1
CONVENTIONAL TURBINE AND MHD POWER GENERATION	1
COMPARISON OF EFFICIENCIES	4
THE NEED FOR PREHEATED AIR	5
DIRECT AND INDIRECT-FIRED AIR PREHEATERS	6
GENERAL AIR PREHEATER DESIGN	8
MODEL DEVELOPMENT AND DESIGN OF FALLING-PARTICLE AIR PREHEATER	14
INTRODUCTION	14
PREDICTION OF MATERIAL PROPERTIES	14
GENERAL DESIGN CONSIDERATIONS	15
PARTICLE SIZE DISTRIBUTION	16
PARTICLE TERMINAL VELOCITIES AND CHAMBER DIAMETER	17
DETERMINATION OF INSULATION THICKNESS	17
OVERALL HEAT LOSS TO SURROUNDINGS	18
DEVELOPMENT OF MODEL DESIGN COMPUTER PROGRAM	20

TABLE OF CONTENTS (Cont).

	Page
MODEL DEVELOPMENT AND DESIGN OF CORED-BRICK AIR PREHEATER	21
COST SUMMARY FOR INDIRECT-FIRED AIR PREHEATERS	23
FALLING-PARTICLE AIR PREHEATERS	23
CORED-BRICK AIR PREHEATERS	24
FUEL SOURCES FOR INDIRECT-FIRED AIR PREHEATERS	25
INTRODUCTION	25
COAL CARBONIZATION	25
COAL GASIFICATION	26
OVERALL INDIRECT-FIRED AIR PREHEAT SYSTEMS COST COMPARISON	30
CAPITAL COST COMPARISON	30
ANNUAL COST ESTIMATION	30
COMMENTS	33
CAPITAL COST COMPARISON OF DIRECT AND INDIRECT-FIRED AIR PREHEAT SYSTEMS	33
COMMENTS	33
APPENDICES	35
APPENDIX A: PREDICTION OF MATERIAL PROPERTIES	36
1. CONSTITUENTS OF COAL GAS, MOLE %	36
2. PRODUCTS OF COAL GAS COMBUSTION	36
3. HOT EXHAUST GAS PROPERTIES	37
4. HOT AIR PROPERTIES	38

TABLE OF CONTENTS(Cont).

Page

5. ALUMINA PARTICLE PROPERTIES. 38

6. INSULATION DATA. 38

7. MHD COAL EXHAUST GAS PROPERTIES. 39

APPENDIX B: GENERAL DESIGN BALANCES. 41

1. COMPOSITION OF MONTANA SUB-BITUMINOUS COAL 41

2. AIR INPUT TO 400 MW(T) MHD COMBUSTOR 41

3. HEAT TRANSFER RATE TO AIR IN PREHEATER 42

APPENDIX C: MODEL DEVELOPMENT OF FALLING-PARTICLE AIR PREHEATER. 43

1. PARTICLE SIZE DISTRIBUTIONS. 43

2. TERMINAL VELOCITY AND CHAMBER DIAMETER CALCULATION . . . 43

3. DETERMINATION OF INSULATION THICKNESS. 45

4. WALL HEAT LOSS DETERMINATION 47

5. OVERALL HEAT LOSS DETERMINATION. 47

6. DEVELOPMENT OF DESIGN EQUATIONS. 49

7. DEFINITIONS OF PROGRAM VARIABLES AND PROGRAM LISTING . . 53

APPENDIX D: MODEL DEVELOPMENT OF CORED-BRICK AIR PREHEATER . . . 65

APPENDIX E: COST PREDICTION FOR FALLING-PARTICLE AIR PREHEATER . 72

1. INSULATION COSTS 72

2. STEEL COLUMN COST. 72

3. ALUMINA PARTICLE COST. 74

4. MISCELLANEOUS CAPITAL COSTS. 74

TABLE OF CONTENTS (Cont).

Page

5. ESTIMATION OF ANNUAL MAINTENANCE COSTS 75

APPENDIX F: COST PREDICTION FOR CORED-BRICK AIR PREHEATER. . . . 76

1. INSULATION COSTS 76

2. STEEL COLUMN COSTS 76

3. CORED-BRICK COST. 77

4. MISCELLANEOUS CAPITAL COSTS 77

5. ESTIMATION OF ANNUAL MAINTENANCE COSTS. 78

APPENDIX G: DESIGN DATA FOR COAL CARBONIZATION SYSTEM 79

1. MASS AND ENERGY BALANCES. 79

APPENDIX H: DESIGN DATA FOR COAL GASIFICATION SYSTEM. 81

1. MASS AND ENERGY BALANCES. 81

2. CAPITAL AND ANNUAL COST PREDICTION. 82

BIBLIOGRAPHY 83

LIST OF TABLES

TABLE		PAGE
I	FALLING-PARTICLE CHAMBER DIMENSIONS.	21
II	CORED-BRICK CHAMBER DIMENSIONS	22
III	ESTIMATED CAPITAL COST OF AN INDIRECT-FIRED FALLING-PARTICLE AIR PREHEATER	23
IV	ESTIMATED CAPITAL COST OF AN INDIRECT-FIRED CORED-BRICK AIR PREHEATER.	24
V	COST COMPARISON OF OVERALL INDIRECT-FIRED CORED-BRICK AND FALLING-PARTICLE AIR PREHEAT SYSTEMS.	31
VI	CAPITAL COST COMPARISON OF DIRECT AND INDIRECT-FIRED AIR PREHEAT SYSTEMS.	33

LIST OF FIGURES

FIGURE		PAGE
1	CONVENTIONAL TURBINE AND MHD POWER GENERATION SYSTEMS COMPARISONS.	2
2	COMPARISON OF DIRECT AND INDIRECT-FIRED AIR PREHEAT SYSTEMS.	7
3	CROSS-SECTION OF A CORED-BRICK AIR PREHEATER	10
4	SIMPLIFIED SCHEMATIC OF FALLING-PARTICLE AIR PREHEATER . . .	12
5	COLUMN INSULATION CROSS-SECTION.	19
6	AIR PREHEAT SYSTEM WITH COAL CARBONIZER AS FUEL SOURCE . . .	27
7	AIR PREHEAT SYSTEM WITH COAL GASIFIER AS FUEL SOURCE	28
8	ENTHALPY OF MHD COAL EXHAUST GAS vs. TEMPERATURE	40

NOMENCLATURE

(Excludes terminology used exclusively in computer program. See Appendix C-7 for definitions of program variables).

SYMBOL	EXPLANATION	UNITS
A	particle surface area	ft^2
A_c	particle cross-sectional area	ft^2
C_D	drag coefficient	dimensionless
C_p	specific heat (constant pressure)	$BTU/lb_m°F$
D_c	inside column diameter	ft
F_d	drag force	lb_f
N_T	total number of holes in cored-brick column	
Nu	Nusselt number, hD/k	dimensionless
Pr	Prandtl number, $C_p\mu/k$	dimensionless
R	heat transfer resistance	°F hr/BTU
Re	Reynolds number, $Du_b\rho/\mu$	dimensionless
St	Stanton number, Nu/RePr	dimensionless
T_w	outside wall temperature	°R
T_s	particle temperature	°R
T_g	gas temperature	°R
T_∞	ambient temperature	°R
U_o	overall heat transfer coefficient	$BTU/hrft^2°F$
d_o	hole diameter in cored-brick	ft

NOMENCLATURE (Cont)

SYMBOL	EXPLANATION	UNITS
d_p	particle diameter	ft
f	friction factor	dimensionless
g	acceleration of gravity	ft/sec^2
g_c	gravitational constant, 32.17	$ftlb_m/lb_f sec^2$
h	convective heat transfer coefficient	$BTU/hrft^2°F$
k	thermal conductivity	BTU/hrft°F
q	heat transfer rate	BTU/hr
U_A	gas velocity	ft/sec
U_T	particle terminal velocity	ft/sec
V	particle velocity	ft/sec
W_g	gas mass flow rate	lb_m/hr
W_s	particle mass flow rate	lb_m/hr
X	vertical distance from top of column	ft
δ	insulation thickness	ft
μ	viscosity	$lb_m/ftsec$
ρ_g	gas density	lb_m/ft^3
ρ_s	particle density	lb_m/ft^3
θ	time	sec
τ_w	shear stress at wall	lb_f/ft^2
ΔX	incremental change in X	ft
ΔP	pressure drop	lb_F/in^2

ABSTRACT

A preliminary design for an indirect-fired falling-particle air preheater for a 400 MW (thermal) MHD power generation plant was made. The project was broken down into three major parts: material properties prediction, development of a theoretical model, and capital and annual cost estimation of the overall design.

A theoretical model was developed for an indirect-fired cored-brick air preheater. Capital and annual costs were estimated and compared to those of the falling-particle air preheater. It was found that overall air preheat systems involving these two designs would have approximately the same capital costs of $\sim$ \$44 x 10^6, and annual costs of $\sim$\$6 x 10^6.

An economic comparison was then made between overall indirect-fired air preheat designs, and overall direct-fired designs. In both the falling-particle and cored-brick cases, the capital cost of the indirect-fired design was approximately 50% greater than the capital cost of the direct-fired design.

INTRODUCTION

CONVENTIONAL TURBINE AND MHD POWER GENERATION

Magnetohydrodynamic (MHD) power conversion is a method of generating electricity with features similar to those of a conventional steam tubrine driven generator. These similarities will be discussed, and then features peculiar to MHD power conversion will be discussed.

Figure 1 illustrates a very simplified steam turbine driven generator and a MHD generator. In the case of the steam turbine generator, the thermal energy of hot combustion products (formed by the burning of some fossil fuel) is transformed into latent energy by vaporizing water to steam. The transformation to mechanical energy is accomplished by expanding the steam against turbine blades. Finally, the turbine shaft rotates a conductor (the armature) in a stationary magnetic field (the stator). As the lines of magnetic flux are broken, a net electromotive force and resulting current flow is created in accordance with Faraday's laws of induction. It should be pointed out that the working gas in the turbine could be any hot, high pressure gas, as well as steam.

The MHD power conversion system has a number of similarities to the turbine generator. In the MHD case, the conductor which breaks the lines of magnetic force of the stationary magnetic field is a hot, electrically conducting fluid, usually a gas. Thus the thermal energy of the conducting fluid is transformed directly to electrical energy. The system consists of an expanding duct through which the hot gas flows, which is lined on two opposite sides with electrodes. The electrodes

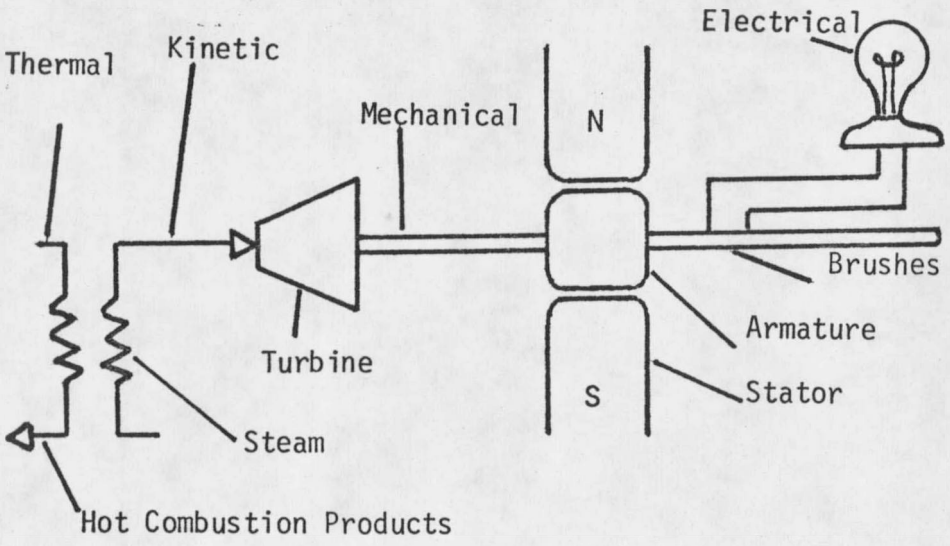

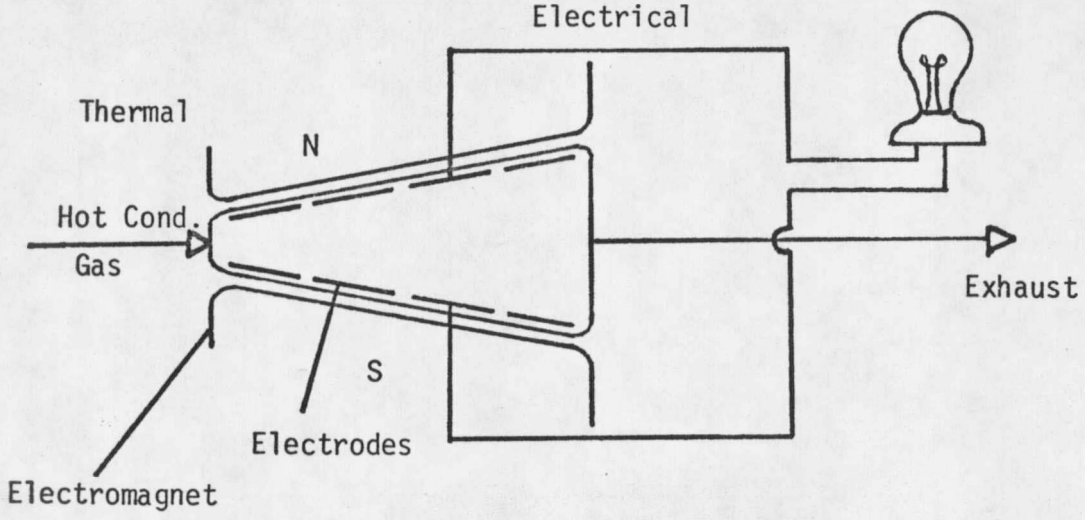

FIGURE 1. CONVENTIONAL TURBINE AND MHD POWER GENERATION SYSTEMS COMPARISONS

carry the current to the external load circuit in the same fashion as the brushes in the conventional generator.

It should be noted here that the rotational motion of the armature in a conventional generator creates a alternating current, whereas the continuous motion of the gas past the electrodes in an MHD generator creates direct current.

The two types of MHD systems possible are open cycle and closed cycle. In the closed cycle case, the conducting fluid is recycled and regenerated through the use of heat exchangers. Examples of this type of system are cycles involving noble gases, and liquid metals. In the open cycle case, the conducting fluid passes through the MHD duct only once. Since this paper is directed toward the design of heat exchange components for open cycled fossil-fueled MHD systems the closed cycle system will not be discussed further.

In an open cycle MHD system, the hot gas (combustion products of some fossil fuel) is made an electrical conductor by the addition of a seed, such as K_2O or K_2CO_3. The low ionization potential of the seed enables a free flow of electrons within the gas. A conducting gas of this type is called a plasma. The electrical conductivity of the gas is a relative measure of the ease in which the gas will conduct electricity. The optimum seed concentration is about 1-5% by weight (1,2).

COMPARISON OF EFFICIENCIES

In the type of power conversion systems discussed so far, thermodynamic efficiency is optimized by maximizing the temperature of the working gas. The presence of highly stressed moving parts in a turbine generator becomes the limiting factor in the working gas temperature, and thus in the generator efficiency. As a result of this, the electrical efficiencies obtained in conventional steam turbine power plants is between 30-45%. In the case of MHD systems, no moving or highly stressed parts are present, and all parts are readily accessible to external cooling. Thus the limiting factor in MHD efficiency is the temperature of the working gas itself, which can be much higher than the maximum temperature in a turbine. It is foreseen that working gas temperatures as high as 5000-6000°F are possible for MHD applications. Efficiencies of systems employing present technology are predicted to be about 50%. Advanced systems are foreseen to have efficiencies as high as 60%. As a further comparison the average efficiency of a nuclear fission power generating facility is 32%. Thus an advanced MHD plant would have 1.5 times the efficiency of a conventional steam turbine plant, and 1.9 times the efficiency of a conventional nuclear plant. It should be noted here that the advantage of an MHD system is not is high efficiency alone, but its ability to convert thermal to electrical energy in much higher temperature ranges than turbine generators. As a result, the exhaust gases from the MHD duct would be transferred to a conven-

tional gas or steam turbine generating facility, or "bottoming" plant. The total power output of the facility would be about evenly divided between the MHD plant and the bottoming plant (1,3).

THE NEED FOR PREHEATED AIR

The working gas temperatures necessary for efficient MHD power generation are well above gas temperatures accessible by conventional combustion methods. The combustion of coal with ambient air gives a maximum temperature of about 3000°F. However, efficient MHD power generation requires a temperature of about 5000°F. Two methods are available in achieving this temperature. The first is the use of excess oxygen. In view of the high cost of a facility capable of producing the amounts of oxygen which would be necessary for a commercial scale MHD installation, this method is looked upon as uneconomical with present technology. The second method involves preheating the combustion air before it is used to burn the coal. This method has been used extensively in the steel industry. Conventional tube and shell heat exchangers can be used to preheat air to about 1700°F. To reach the temperature necessary for MHD power generation, an air preheat temperature of about 3100°F is required. Thus a heat exchange system is needed which will raise the temperature of air from 1700°F to 3100°F. A number of systems are presently being looked at.

DIRECT AND INDIRECT-FIRED AIR PREHEATERS

Air preheaters are of two basic types according to how they fit into the overall MHD process - direct-fired and indirect-fired, as shown in Figure 2. The direct-fired air preheater utilizes the thermal energy of the MHD exhaust gas, which leaves the MHD duct at about 3300°F, to directly preheat air. The indirect-fired air preheater utilizes the thermal energy of exhaust from a separately fired clean fuel combustor to preheat the combustion air. The direct-fired design has three basic disadvantages. First, the MHD exhaust is laden with vaporized seed and slag, both of which are highly corrosive. Second, as the exhaust gas transfers heat in the air preheater, both the seed and slag condense, coating the internal works of the preheater. This solid residue would have to be continuously removed, not only from an operations standpoint, but also because the cost of the seed makes recycle imperative. Third, the inlet pressure to the MHD duct must be ∿8 atm in order that the gas can push itself through the duct. As a result of this, the preheated combustion air must be pressurized to 8 atm. However, the outlet pressure from the MHD duct is ∿1½ atm. Thus, there will be a pressure differential of ∿6½ atm. between the exhaust gas side and the air side of the preheater. The indirect-fired air preheater has none of these disadvantages. Since the fuel is clean, no problems with seed and slag are encountered. Also, since the inlet pressure of the combustion products of the fuel can be arbitrarily set, the hot gas side and the

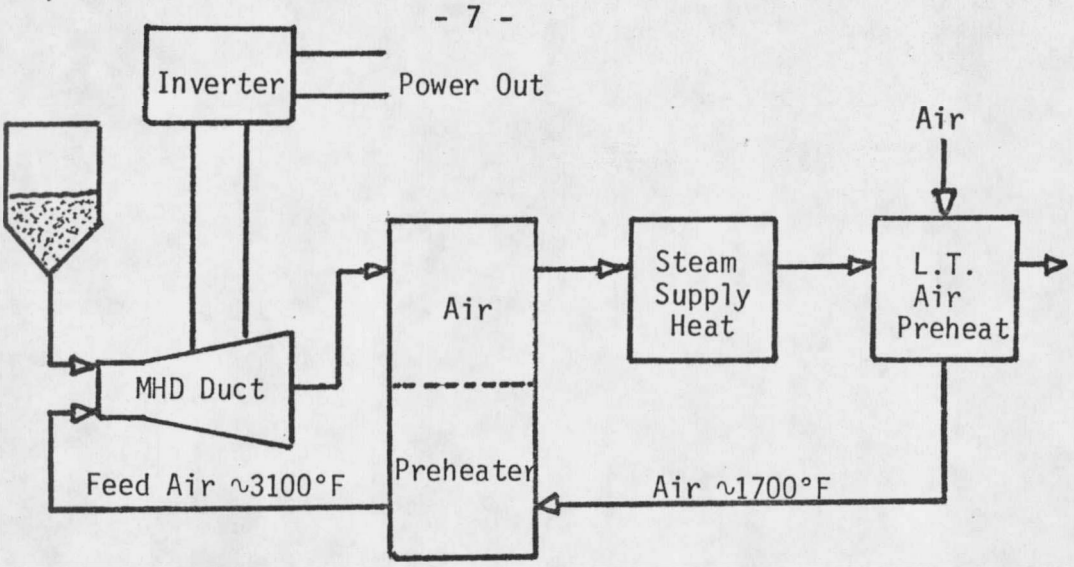

DIRECT-FIRED AIR PREHEATER

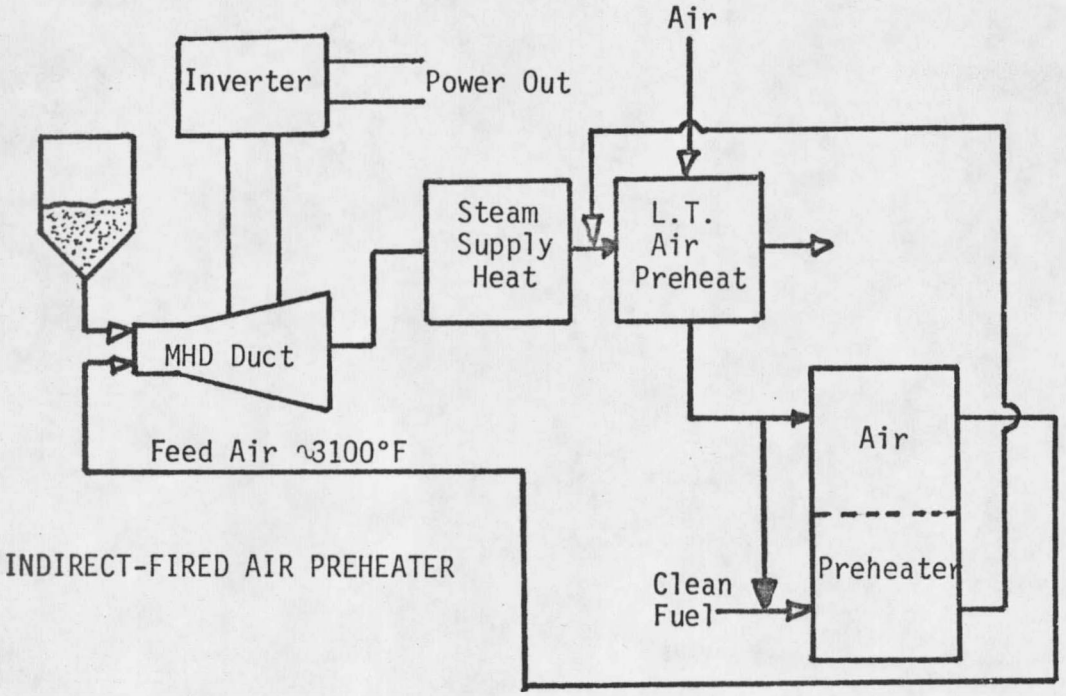

INDIRECT-FIRED AIR PREHEATER

FIGURE 2. COMPARISON OF DIRECT AND INDIRECT-FIRED AIR PREHEAT SYSTEMS

air side of the preheater can be run at a 1:1 pressure ratio. The main disadvantage of the indirect-fired air preheater is that, since a separate clean fuel must be employed, $\sim$ 2 points in overall cycle efficiency will be lost (5,8). Also the need for a clean fuel is a disadvantage.

GENERAL AIR PREHEATER DESIGN

Since conventional low-temperature heat exchange materials and design are inadequate for high-temperature air preheater applications, new materials and designs must be considered. Materials most likely to be able to withstand high-temperature corrosion and thermal stress are of the refractory type. The material used for the heat-transfer medium should have a high thermal conductivity and heat capacity for efficient heat transfer. The three most popular candidates, in order of increasing cost, are alumina (Al_2O_3), magnesia (MgO), and zirconia (ZrO_2). Materials of this type are employed in the design of both the heat transfer medium and the external insulation of the air preheater.

Of the many air preheater designs presently being researched, two will be focused upon. These are the cored-brick air preheater, and the falling-particle air preheater.

The cored-brick air preheater is basically an insulated column packed with longitudinally cored refractory bricks of high heat capacity. A cross-section of a typical cored-brick air preheater is shown in

Figure 3. The separate bricks are of hexagonal cross-section and the core diameter ranges from 0.25 inches to 0.75 inches (4,11). The method of operation is as follows: the air preheater column is suitably valved at each end so that hot gas or air can alternatively be run through the column, in countercurrent directions. Initially, the cored bricks are heated for a specified period of time by hot gas. Then air is heated by running it through the column, also for a specified amount of time. A problem is that the air output is of a cyclic nature, while the MHD process requires a constant flow rate of combustion air. This problem is solved by the use of a number of cored-brick air preheaters operating in a continuous cycle to output a constant air flow rate and temperature. The greatest amount of heat transfer per unit volume (and therefore the highest air preheat temperature) is obtained with the smallest flow passage diameter, 0.25 inches. This presents no problem in the indirect-fired case. However, in the direct-fired case, clogging of the flow passages by condensing seed and slag requires that the passage diameter be on the order of 0.75 inches for effective operation. Thus, for a given air preheat temperature, the direct-fired air preheater will be of considerably larger size than the indirect-fired air preheater. An important point is that thermal expansion of refractory materials in these temperature ranges is considerable, and must be accounted for in the overall column design (4,5).

The falling-particle air preheater is shown by simplified schematic

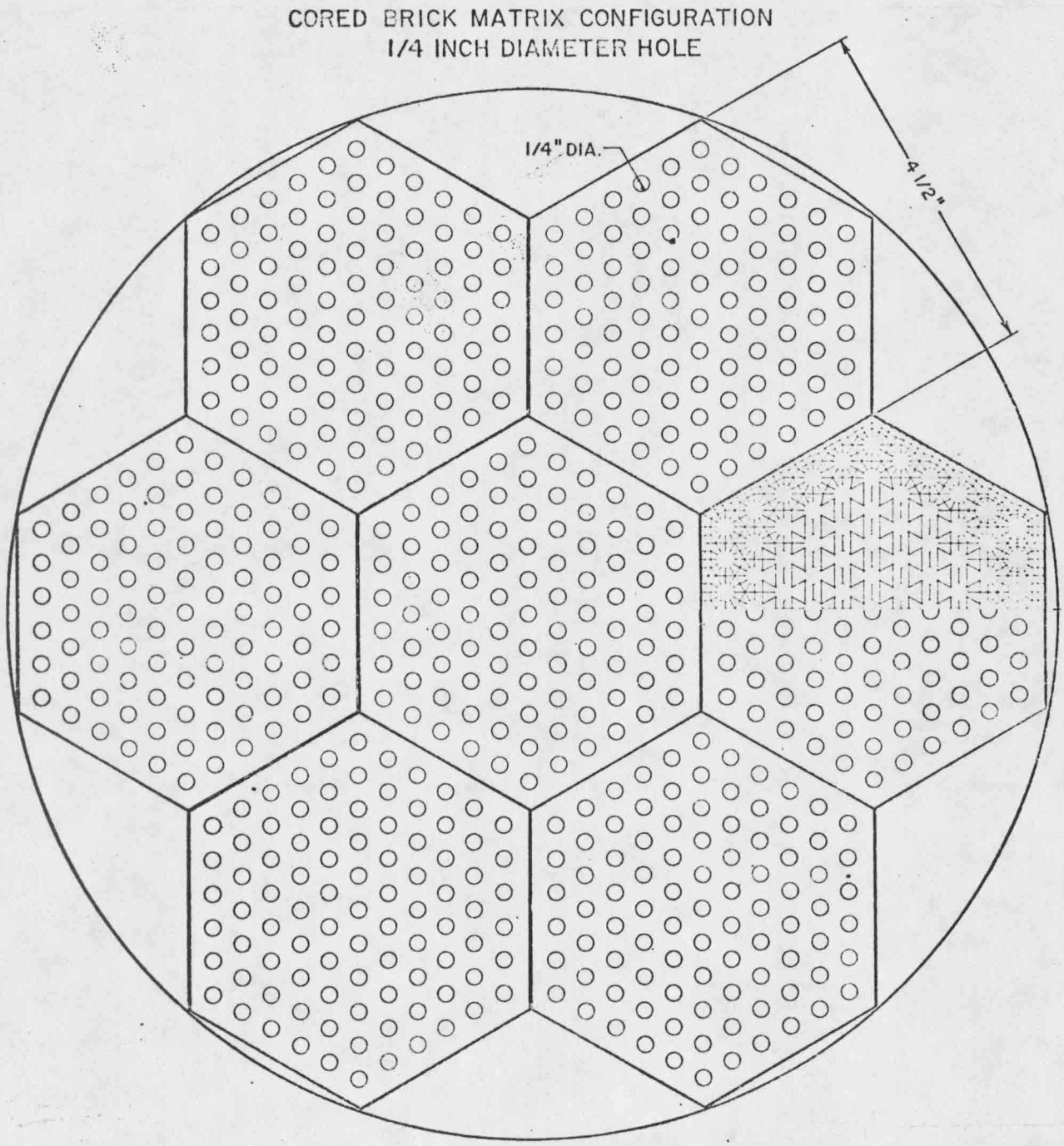

FIGURE 3. CROSS-SECTION OF A CORED-BRICK AIR PREHEATER

in Figure 4. The design consists of two vertical columns, one above the other. Small (∿ 0.05 inch diameter) refractory particles fall through the upper chamber, are held up at the interface between the chambers, and then fall through the lower chamber. The particles are then returned to the top of the upper chamber by a pneumatic blower, completing the cycle. At the top of each chamber is a distributor plate which spreads the particles evenly across the chamber diameter. Hot gas (the heating fluid) enters the bottom of the upper chamber, flows up the chamber countercurrent to the flow of particles, and exits at the top of the chamber through an exhaust manifold. As the gas flows past the particles, thermal energy is transferred to the particles. In similar fashion, air enters the bottom of the lower chamber, flows upward countercurrent to the particle flow, and exits through an exhaust manifold. As the air flows past the heated particles, thermal energy is transferred to the air. It should be noted here that the design shown in Figure 4 is specific for the indirect-fired case. Since both the upper and lower chambers are at nearly the same pressure (∿ 8 atm), the weight of a number of feet of particles at the interface between the chambers should offset any leakage of air or hot gas. However, since such a large pressure differential exists between the upper and lower chambers in the direct-fired case, a complex valving mechanism of some sort must be devised to permit continuous flow of particles from the upper to lower chamber, and minimize air leakage. Unlike the cored-

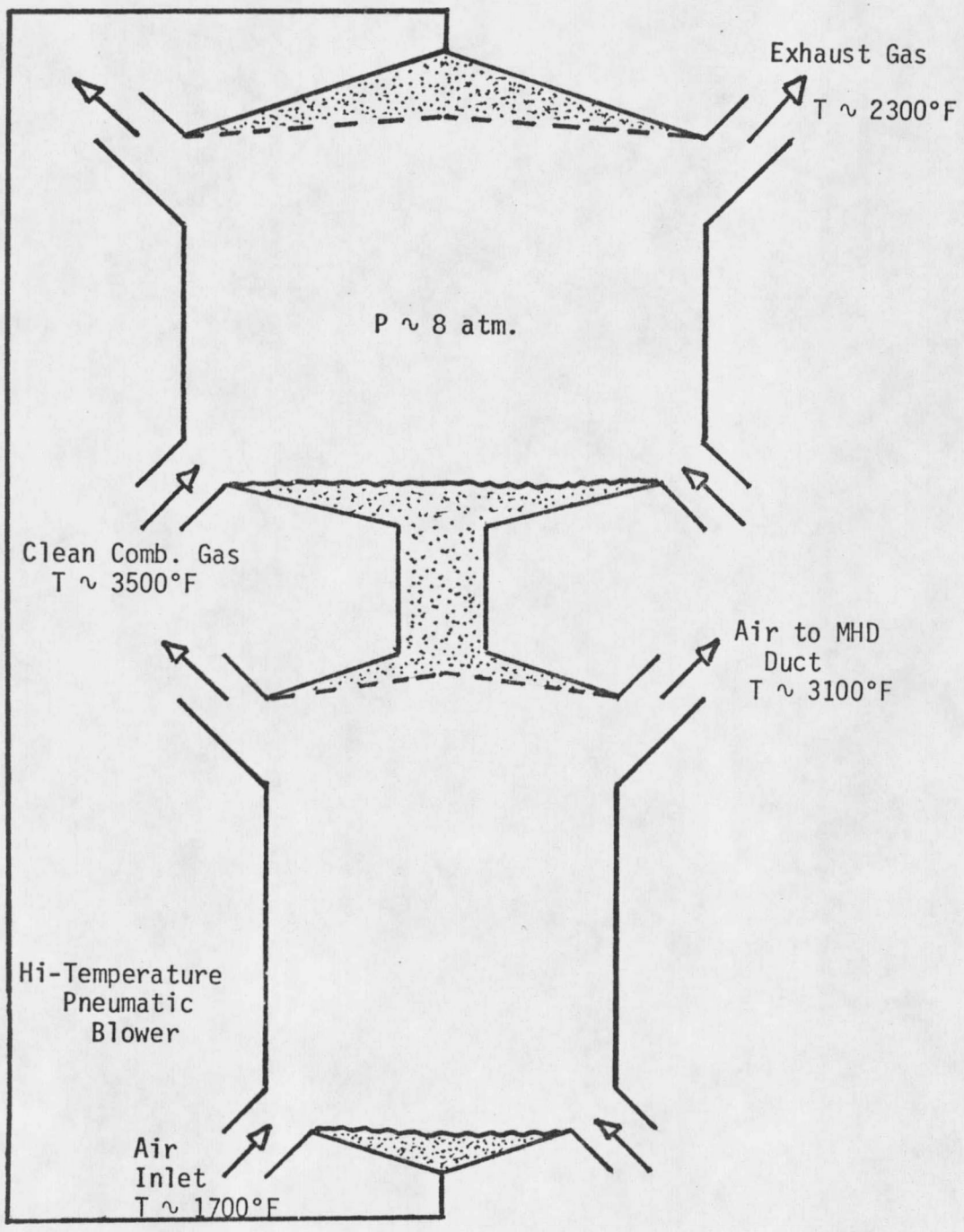

FIGURE 4. SIMPLIFIED SCHEMATIC OF FALLING-PARTICLE AIR PREHEATER

brick air preheater, the falling particle air preheater is a continuous process, outputting a constant flow rate and temperature of combustion air. Thus, cyclic operation and its complex valving are unnecessary.

MODEL DEVELOPMENT AND DESIGN OF FALLING-PARTICLE AIR PREHEATER

INTRODUCTION

A theoretical model of the falling particle air preheater was assembled on computer by W. E. Genetti. A preliminary design was then made based on the results of the model data. This thesis deals specifically with the design of an indirect-fired falling particle air preheater. Also, a design for an indirect-fired cored-brick air preheater was made. The two designs are compared from both a structural and cost viewpoint. In addition, a cost tradeoff analysis is made for both the falling-particle and cored-brick designs between the indirect-fired and the direct-fired cases. Design and cost data for direct-fired air preheaters were provided by W. E. Genetti and R. L. Mussulman.

PREDICTION OF MATERIAL PROPERTIES

As a prelude to model development of the air preheater, equations were developed to predict the general properties of the materials involved in the design for the necessary temperature and pressure ranges. The materials include the hot exhaust gases (heating fluid), air (heated fluid), falling refractory particles, and insulation.

As mentioned earlier, a separate clean fuel is needed to fire the air preheater. This fuel could be fuel oil, natural gas, or a fuel produced from the devolatilization of coal. In view of the cost and availability of fuel oil and natural gas, a fuel produced from coal

devolatilization was called for in the original design. This fuel is produced by the heating of coal to around 2000°F in the absence of air, driving off the volatile matter as a gas with a heating value of about 575 BTU/ft^3. This process is also called carbonization. Carbonization of 2000 lb of coal yields about 11,000 ft^3 of coal gas, plus about 1400 lb of coke. The constitutents of the coal gas and its products of combustion are presented in Appendix A.

Equations for the following general properties for air and the hot exhaust gases were developed: viscosity, thermal conductivity, and heat capacity, all as a function of temperature, and density as a function of temperature, and pressure. These equations, along with other pertinent material properties are presented in Appendix A.

GENERAL DESIGN CONSIDERATIONS

All preheater design work, both for this report and for the Genetti-Mussulman design, was done on the basis of a 400 megawatt (thermal) MHD power generation facility. The thermal power rating is defined as the power input to the MHD duct. The stoichiometry of the MHD combustion reaction and its related mass balances are presented in Appendix B-1. As is evidenced by the air requirement for the combustion reaction, the air preheater must supply 1.279 x 10^6 lb_mair/hr to the combustor. As previously mentioned, the temperature of the preheated air must be about 3100°F.

Since conventional shell-and-tube heat exchangers are capable of producing air temperatures of 1700 F, this is assumed to be the air inlet temperature of the air preheater. With these parameters set, the heat transfer rate to the air in the preheater can be calculated (Appendix B-3). This was found to be 5.155×10^8 BTU/hr. It should be noted at this point that this design for a 400 MW heat exchange facility calls for three air preheater columns, two running simultaneously in parallel, and one spare. Thus, for one column, the air flow rate would be 6.395×10^5 lb/hr and the heat transfer rate to the air would be 2.578×10^8 BTU/hr.

PARTICLE SIZE DISTRIBUTION

The next step in model development was to obtain a realistic size distribution of the alumina particles. It was found that the tabular alumina stock supplied by the Aluminum Company of America would have to be classified, narrowing the particle size distribution down to usable ranges. Two particle size ranges were investigated. In either case, the largest particle diameter is 0.05 in. The wide distribution is 0.038-0.05 in. diameter, and the narrow distribution is 0.042-0.05 in. diameter. These distributions will be referred to as "blowouts", since any particle smaller than the included range would blow out the top of the chamber. These two particle size distributions are listed in Appendix C-1.

PARTICLE TERMINAL VELOCITIES AND CHAMBER DIAMETER

The inside diameter of the chamber is a function of the terminal velocity of the particles. The terminal velocity of a particle is defined as that velocity at which the falling particle stops accelerating. In other words, since drag increases as velocity increases, it is the maximum attainable velocity of the particle in a given fluid. The terminal velocities of the smallest particles were calculated, since they would be the first to "blow out". The maximum gas velocity (at maximum temperature) was then taken to be 100% of this terminal velocity. Thus, since the air mass flow rate is known, the air chamber diameter can be calculated. These calculations are presented in Appendix C-2.

At this point, it was initially assumed that chamber heat losses were zero; thus $q_{air} = q_{gas}$. In this manner, a gas mass flow rate was found and gas chamber diameter calculated in analogous fashion to the air chamber diameter, as presented in Appendix C-2. The gas mass flow rate is 6.52×10^5 lb/hr. The inside diameters of the gas and air chambers are, respectively, 14.2 feet and 11.1 feet (for the 0.042 inch blowout case).

DETERMINATION OF INSULATION THICKNESS

The thickness of insulation needed to effectively insulate the column was now determined. Properties of the insulation used are presented in Appendix A-6. A trial-and -error solution to the insulation

thickness was made following the procedure presented in Appendix C-3, with the limiting condition that the maximum outer wall temperature should not be above $\sim$ 250°F. The resulting wall cross-section, having an overall thickness of 3.5 feet, is shown in Figure 5.

OVERALL HEAT LOSS TO SURROUNDINGS

With the wall cross-section known, the rate of heat loss through the wall can now be determined. The heat transfer equation developed in Appendix C-3 is used to find the outer wall temperature at various values of gas temperature. Then (q/A) loss is found at each of these temperatures, and a curve is fit to the data. The resulting equation is $(q/A)_{loss}$ as a function of Tg. These calculations are related in Appendix C-4.

Overall air preheater heat losses can now be calculated. The overall losses are assumed to be the sum of the heat losses in the air and gas chambers, plus the heat loss from the particle recycle system. The following two assumptions must be made:

1. The heights of the gas and air chambers are 20 feet and 30 feet, respectively.
2. The heat loss from the particle recycle system is approximated by the arithmetic average of the heat losses from the gas and air chambers.

This procedure is outlined in Appendix C-5. With the overall heat

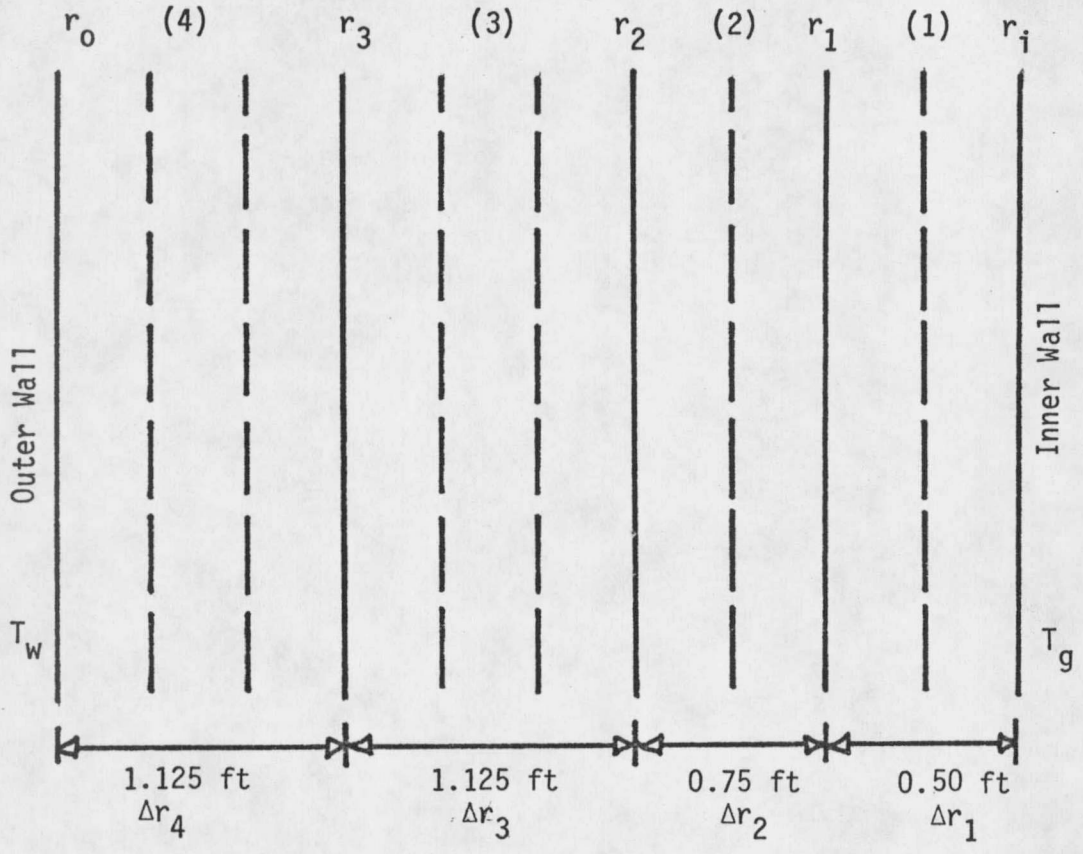

(1) Norton AH-199B

(2) Norton AN-599

(3) Johns-Manville JM-3000

(4) Johns-Manville JM-23

FIGURE 5. COLUMN INSULATION CROSS-SECTION

loss known, the amount of heat transferred from the hot gas to the particles can be determined, and a refined value for the gas exit temperature is found to be 2330°F. The average particle temperature between the chambers is assumed to be the average of the bottom gas temperature and the top air temperature, or 3300°F. The average particle temperature in the particle recycle system is specified to be the average of the top gas temperature and the bottom air temperature, or 2015°F. This method of estimating the chamber heights to arrive at the overall heat losses is assumed to be rigorous, since heat losses amount to only $\sim$ 0.2% of the total heat transfer rate.

Now that all heat transfer rates are known, the particle mass flow rate is calculated to be 6.54×10^5 lb/hr.

DEVELOPMENT OF MODEL DESIGN COMPUTER PROGRAM

A computer program was developed to assist in the preliminary design of the air preheater. The operation of the program involves the solution of three simultaneous differential equations: an energy balance between particles and air across a differential element of time, a momentum balance on a falling particle, and an overall energy balance, including heat losses, across a differential column element. These balances are developed in Appendix C-6. Definitions of all program variables, a program listing, and a program output are presented in Appendix C-7. As can be seen, the program output gives a listing of

important chamber parameters in increments of height, starting at the top of the gas or air column and moving down. Based on this data and data already presented, overall chamber dimensions can be calculated. These are listed in Table I.

TABLE I. FALLING PARTICLE CHAMBER DIMENSIONS

	Gas Chamber		Air Chamber	
Blowout (in.)	.038	.042	.038	.042
Inside Diameter (ft)	15.1	14.2	11.84	11.1
Outside Diameter (ft)	22.1	21.2	18.84	18.1
Chamber Height (ft)	20.5	14.2	39.8	30.0
Gas Mass Flow Rate (lb/hr)	6.52×10^5	6.52×10^5	6.395×10^5	6.395×10^5
Max. Gas Velocity (ft/sec)	18.9	21.5	18.34	20.88
Gas Inlet Temperature (°F)	3500	3500	1700	1700
Gas Exit Temperature (°F)	2330	2330	3100	3100

MODEL DEVELOPMENT AND DESIGN OF CORED-BRICK AIR PREHEATER

A model was developed to size an indirect-fired cored brick air preheating system. It is assumed that a 400 megawatt (thermal) power generation facility would require an air preheater system consisting of seven separate cored brick chambers, six on line with one spare. At any given time, two columns would be heating air or be being heated by

hot gas. The model consists of an energy balance across a differential element of chamber area, assuming the bricks to be isothermal. For the indirect-fired case, bricks with 0.25 inch diameter holes are used. This hole size gives the bricks a cross-sectional geometric porosity of 25%. Convective heat transfer data (17) for heat transfer coefficients in circular tubes is used. Pressure drop, as well as volume, must be optimized to give the best design. Model development is presented in Appendix D. An insulation thickness of 3.5 ft is assumed. The chamber dimensions resulting from this model are presented in Table II.

TABLE II. CORED BRICK CHAMBER DIMENSIONS

Hole Diameter (in.)	0.25
Overall Height (ft)	23.3
Inside Diameter (ft)	8.9
Outside Diameter (ft)	15.9
ΔT_{av} - Air Flow (°F)	155
ΔT_{av} - Gas Flow (°F)	100
Pressure Drop, psi	4.43

COST SUMMARY FOR INDIRECT-FIRED AIR PREHEATERS

FALLING-PARTICLE AIR PREHEATERS

Capital cost prediction for the indirect-fired falling-particle air preheater is developed in Appendix E. These costs are for one unit only. Table III gives cost data for both one unit and for an overall three-unit system.

TABLE III. ESTIMATED CAPITAL COST OF INDIRECT-FIRED FALLING-PARTICLE AIR PREHEATER

	0.038 in. Blowout		0.042 in. Blowout	
	Unit Cost	Total Cost*	Unit Cost	Total Cost*
Steel	$2.27x10^6	$6.81x10^6	$1.72x10^6	$5.2x10^6
Insulation	1.73x10^6	5.19x10^6	1.33x10^6	5.0x10^6
Alumina Particles	.12x10^6	.36x10^6	.15x10^6	.45x10^6
Piping	.3x10^6	.9x10^6	.3x10^6	.9x10^6
Valves	1.36x10^5	.41x10^6	.136x10^6	.41x10^6
Instrumentation		.3x10^6		.3x10^6
Structure		6.2x10^6		4.7x10^6
TOTAL		20.2x10^6		17.0x10^6

* Total Cost of 3 units

CORED-BRICK AIR PREHEATERS

Capital costs for the cored-brick air preheater system are developed in Appendix F. Again, these figures are for one unit only. The overall cored-brick air preheater system consists of seven units. These costs are summarized in Table IV.

TABLE IV. ESTIMATED CAPITAL COST OF INDIRECT-FIRED CORED-BRICK AIR PREHEATER

	Unit Cost	Total Cost (7 units)
Steel	$ .216 x 10^6	$ 1.51 x 10^6
Insulation	.662 x 10^6	4.63 x 10^6
Cored Brick	.552 x 10^6	3.86 x 10^6
Piping		1.1 x 10^6
Valves	.136 x 10^6	.95 x 10^6
Instrumentation		.3 x 10^6
Structure		3.0 x 10^6
TOTAL		$15.4 x 10^6

FUEL SOURCES FOR INDIRECT-FIRED AIR PREHEATERS

INTRODUCTION

A complete indirect-fired air preheater system will necessarily include a fuel source of some sort. Since the purpose of indirect-fired air preheater design is to get away from the disadvantages of using the seed and slag-laden MHD exhaust gas as an energy source, the fuel should be clean and burn efficiently. The three major fuels presently under consideration are fuel oil, natural gas, and synthetic gas made from partially or completely gasified coal. However, in light of the cost and scarcity of fuel oil and natural gas, the cost of running a commercial scale indirect-fired air preheater with these materials would be prohibitive. Thus, the possibility of coal gasification has been concentrated upon. Two basic gasification designs are considered, coal carbonization and coal gasification.

COAL CARBONIZATION

Coal carbonization involves the heating of coal in the absence of air. At a temperature of 1800 - 2000°F, the volatile matter in the coal is driven off as an intermediate-BTU fuel gas, having a heating value of approximately 550 BTU/ft^3 (10). If this gas could be used to fuel the air preheater, then coal would be the sole fuel source of the overall power generation complex. The carbonization of a ton of coal yields approximately 11,000 ft^3 of this fuel gas plus about 1400 lb_m of coke. The coke by-product would be mixed with the coal feed to

the MHD combustor. Mass and energy balances for this system are presented in Appendix G. The carbonizer would be heated by diffused MHD exhaust gases. A simplified design of the system is shown in Figure 6. The balances presented in Appendix G reveal that, even if pure coke were used as the sole fuel source in the MHD combustor, the coke flow rate from the coal carbonizer would be nearly twice the necessary coke flow rate to the MHD combustor. Thus, on this basis alone, the use of coal carbonization to fuel the indirect-fired air preheater appears highly infeasible. Because of this, an economic study of coal carbonization was not pursued.

COAL GASIFICATION

The possibility of using gasified coal as the fuel source for the indirect-fired air preheat system was investigated. The complete gasification of coal to synthetic fuel gas of high BTU content ($\sim$ 950 BTU/ft^3 STD) involves heating the coal to gasify the volatile matter, shift reacting the carbon monoxide with water to form hydrogen and carbon dioxide, removal of H_2S and CO_2, and finally methanation of the resulting gaseous mixture. However, methanation of the CO-H_2 gas mixture has yet to be commercially demonstrated. Thus the gasficiation system will be presented here, but it should be noted that progress is necessary before the system is technologically feasible. Data on the system is presented in Appendix H. Figure 7 depicts a

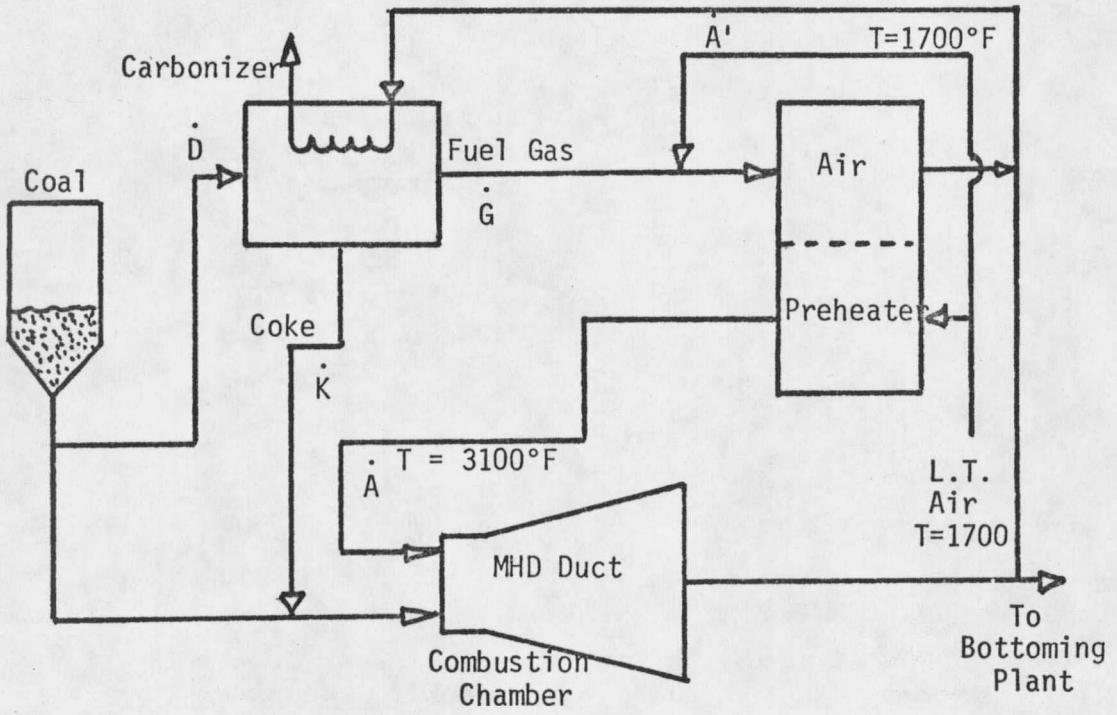

FIGURE 6. AIR PREHEAT SYSTEM WITH COAL CARBONIZATION AS FUEL SOURCE

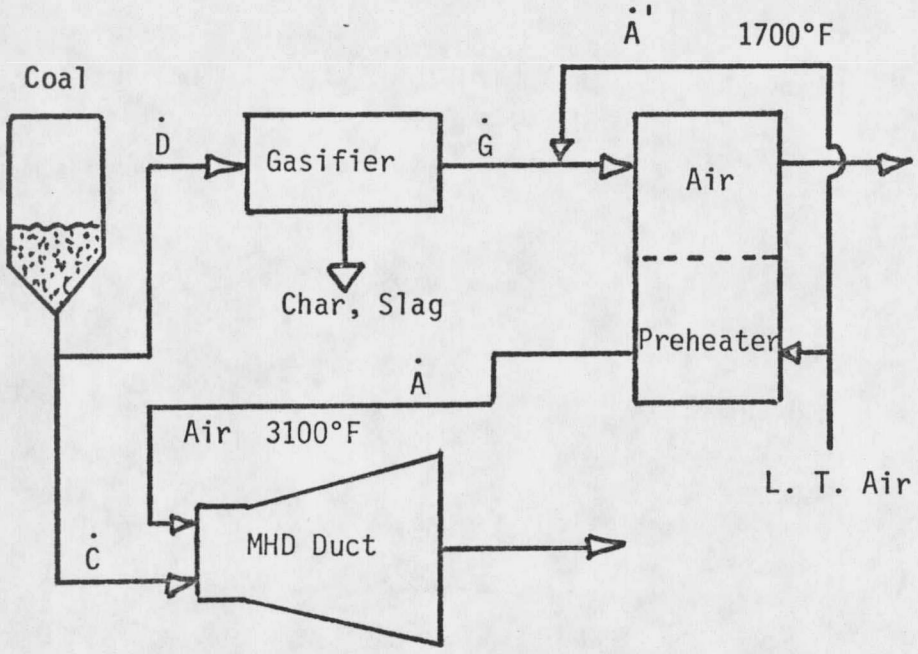

FIGURE 7. AIR PREHEAT SYSTEM WITH COAL GASIFIER AS FUEL SYSTEM

simplified coal gasifier as the fuel source for an indirect-fired air preheater. Data on the possibility of partial char recycle or other uses for char was not available. The particular gasification process investigated is the CO_2-acceptor process, as it has the lowest overall capital cost of all processes looked at. However, it is only capable of gasifying lignite and non-caking sub-bituminous coals. Data was not available on the feasibility of utilizing Montana sub-bituminous coal in the CO_2-acceptor process. As is shown in Appendix H-1, the coal flow rate to the gasifier would be about 47% of the total coal flow rate to the power generating complex. The capital cost for the gasification system is estimated at $\$27.5 \times 10^6$, with an estimated annual operating cost of $\$4.3 \times 10^6$(7).

OVERALL INDIRECT-FIRED AIR PREHEAT SYSTEMS COST COMPARISON

CAPITAL COST COMPARISON

As can be seen in comparing Tables III and IV, the falling-particle preheater (0.042 in blowout) and the cored-brick preheater have nearly the same capital cost, varying by only $\$1.6 \times 10^6$. This is within the limits of estimated accuracy for a long-range economic analysis of this type. Assuming that the capital cost of the fuel source system will be the same for both air preheat systems, overall system capital costs can now be estimated.

ANNUAL COST ESTIMATION

An estimate of annual maintenance costs for the air preheater was made. The development of these costs is presented in Appendix E-5 for the falling-particle air preheater, and in Appendix F-5 for the cored-brick air preheater. It should be noted that these figures are quite rough estimates, and should be weighed with appropriate skepticism. Table V presents an overall capital and annual cost comparison for the two indirect-fired air preheat systems.

TABLE V. COST COMPARISON OF OVERALL INDIRECT-FIRED CORED-BRICK AND FALLING-PARTICLE AIR PREHEAT SYSTEMS

	Cored-Brick Air Preheater	Falling-Particle Air Preheater (0.042 in. Blowout)
Preheater Capital Cost	$ 15.4 x 10^6	$ 17.0 x 10^6
Fuel Source Capital Cost	27.5 x 10^6	27.5 x 10^6
TOTAL Capital Cost	42.9 x 10^6	44.5 x 10^6
TOTAL Annual Cost (includes fuel source)	$ 5.8 x 10^6	$ 6.4 x 10^6

COMMENTS

A number of important points should be made in considering these two overall designs:

1) The level of technology of the cored-brick air preheater design is much higher than that of the falling-particle air preheater design. The utility of the cored-brick design has been demonstrated in a number of applications, and an abundance of design data is available. The falling particle design, however, has not yet been demonstrated.

2) Since the falling-particle design outputs a steady air flow rate at a uniform temperature, operation of the MHD combustor and duct would probably be smoother than with the cyclic

operationg of the cored-brick design.

3) The need for constant-operating valves in the cored-brick will increase annual maintenance costs as a result of valve breakdown and attrition. With the falling-particle design, valves will be used only for startup, shutdown, and flow rate control.

4) Particle replacement through appropriate access ports (probably in the particle recycle system) in the falling-particle design will be a relatively effortless procedure, requiring no equipment shutdown and dismantling. Cored-brick replacement in the cored-brick design, however, will require column shutdown and complete dismantling.

CAPITAL COST COMPARISON OF DIRECT AND INDIRECT-FIRED AIR PREHEAT SYSTEMS

Capital cost data for direct-fired cored-brick and falling-particle air preheat systems was supplied by W. E. Genetti and R. L. Mussulman (12). These data are compared with indirect-fired design data in Table VI. Only the 0.042 in. blowout design of the falling-particle air preheater is considered. Annual cost data for direct-fired air preheat systems was not available.

TABLE VI. CAPITAL COST COMPARISON OF DIRECT AND INDIRECT-FIRED AIR PREHEAT SYSTEMS

	DIRECT-FIRED		INDIRECT-FIRED	
Overall Capital Cost	Falling-Part. 30.4×10^6	Cored-Brick 31.3×10^6	Falling-Part. 44.5×10^6	Cored-Brick 42.9×10^6

As can be seen, in each design case the capital cost of the direct-fired air preheat system is about 75% of the capital cost of the indirect-fired system.

COMMENTS

In comparing the overall designs of direct and indirect-fired air preheat systems, the following comments can be made:

1) Total coal fuel costs for the overall power generating complex with the indirect-fired air preheat system will be

nearly double those of the overall complex with direct-fired air preheat. However, since the thermal energy of the MHD exhaust gas with indirect-fired air preheating is not used to preheat air, a greater percentage of the total power output of the complex will be produced by the bottoming plant. In addition, a larger bottoming plant would be able to utilize the thermal energy of the exhaust gas leaving the indirect-fired air preheat system.

2) Since the environment within the direct-fired system design is much more corrosive than that of the indirect-fired system design, annual maintenance costs can be expected to be substantially higher with the direct-fired system.

3) A few points in overall thermodynamic efficiency are lost in the power generating complex using an indirect-fired air preheat system.(5,8).

APPENDICES

APPENDIX A: PREDICTION OF MATERIAL PROPERTIES

1. Constituents of Coal Gas, Mole %

CO	CO_2	H_2	N_2	O_2	CH_4	Heating Value, BTU/ft^3
8.6	1.5	52.5	3.5	0.3	31.4	575

2. Products of Coal Gas Combustion

	CO_2	H_2O	N_2
Mole %	8.77	21.23	70.00
Weight %	14.15	14.01	71.85

(Ave. Mol. Wt. = 27.28) Flame Temp. = 3665°F

Notes on prediction of exhaust gas and air properties:

a) Viscosity and thermal conductivity of gaseous mixtures were found at given temperatures assuming that:

$$\mu_{mix} = \sum_i y_i \mu_i \qquad k_{mix} = \sum_i y_i k_i$$

where y_i = mole fraction of component i. Viscosities and thermal conductivities were calculated at a number of temperatures. The data were then fit to the following general equations:

$$\mu_{mix} = AT^B \qquad k_{mix} = CT^D$$

b) The heat capacity of the exhaust gas was assumed to obey the following expression:

$$C_{PE} = W_{N_2} C_{PN_2} + X [W_{H_2O} C_{PH_2O} + W_{CO_2} C_{PCO_2}]$$

where W_{N_2}, W_{H_2O}, and W_{CO_2} are the weight fractions of nitrogen, water vapor, and carbon dioxide, respectively. The X is a factor introduced to account for dissociation of H_2O and CO_2 in the gas at high temperatures. X is estimated from heat capacity data calculated for coal combustion gases and the composition of such gases. Since the weight fractions and heat capacities of all gas constituents are known, the factor X can be calculated at a number of temperatures (15).

C_{PE} was calculated for a number of temperatures, and a curve was fit to the resulting data (14,15). A similar procedure was followed by W. E. Genetti in developing the heat capacity equation for hot air.

c) The Ideal Gas Law is assumed accurate in the density equation.

3. Hot Exhaust Gas Properties

Temperature Range: 2000 - 4000°F

$\rho = 37.4\ P/T$ $\quad T = °R,\ P = ATM,\ \rho = lbm/ft^3$

$k = 1.234 \times 10^{-4}\ T^{.778}$ $\quad T = °R,\ k = BTU/hrft°F$

$\mu = 1.52 \times 10^{-7}\ T^{.684}$ $\quad T = °R,\ \mu = lbm/ftsec$

$C_p = -.0260 + 5.100 \times 10^{-6}\ T + 2.967 \times 10^{-8} T^{-2}$ $\quad T = °R,$

$C_p = BTU/lb_m°F$

4. Hot Air Properties

Temperature Range: 1500 - 3500°F

$\rho = 39.12\ P/T$ T = °R, P = ATM, $\rho = lb_m/ft^3$

$k = 4.736 \times 10^{-4}\ T^{.583}$ T = °R, k = BTU/hrft°F

$\mu = 6.07 \times 10^{-7}\ T^{.513}$ T = °R, $\mu = lb_m/ftsec$

$C_p = .2261 + 2.8295 \times 10^{-5}T - 2.286 \times 10^{-9}T^2$

T = °R, C_p = BTU/lb_m°F

5. Alumina (Particle) Properties

Note: The alumina particle used in this design is a tabular alumina product of the Aluminum Company of America. It is 99.5% pure fused alumina. The particle diameter range is 0.036 in - 0.05 in.

$\rho = 232\ lb_m/ft^3$

$k = 2.91 + 2.918 \times 10^{-6}(T-2760)^2 - 1.5611 \times 10^{-12}(T-2760)^4$

T = °R, k = BTU/hrft°F

$C_p = .25667 + 1.6339 \times 10^{-5}\ T$ T = °R, C_p = BTU/lb_m°F

6. Insulation Data

The insulation is of four basic types. This data was supplied by Avco-Everett Research Laboratories, Inc., Everett, Mass (5).

	Mfg.	Type	Thickness in.	k, BTU/hrft°F	Cost, $/ft^3
(1)	Norton	AH-199B	3	1.79	140
(2)	Norton	AN-599	4.5	.894	120
(3)	Johns-Manville	JM-3000	4.5	.292	100
(4)	Johns-Manville	JM-23	4.5	.119	80

7. MHD Coal Exhaust Gas Properties

These properties of the exhaust gas from an MHD duct were developed by W. E. Genetti.

$\rho = 40.946\ P/T$ $\quad T = °R,\quad P = ATM,\quad \rho = lb_m/ft^3$

$k = .000872\ T^{\frac{1}{2}}$ $\quad T = °R,\quad k = BTU/hrft°F$

$\mu = 6.084 \times 10^{-7}\ T^{\frac{1}{2}}$ $\quad T = °R,\quad \mu = lb_m/ftsec$

$C_p = .848446 - .0004834T + 1.01106 \times 10^{-7}T^2$

$T = °R,\quad C_p = BTU/lb_m°F$

8. Following is a graph; Figure 8, of enthalpy of MHD coal exhaust gas vs. temperature, estimated by Avco Everett Research Laboratories Inc.

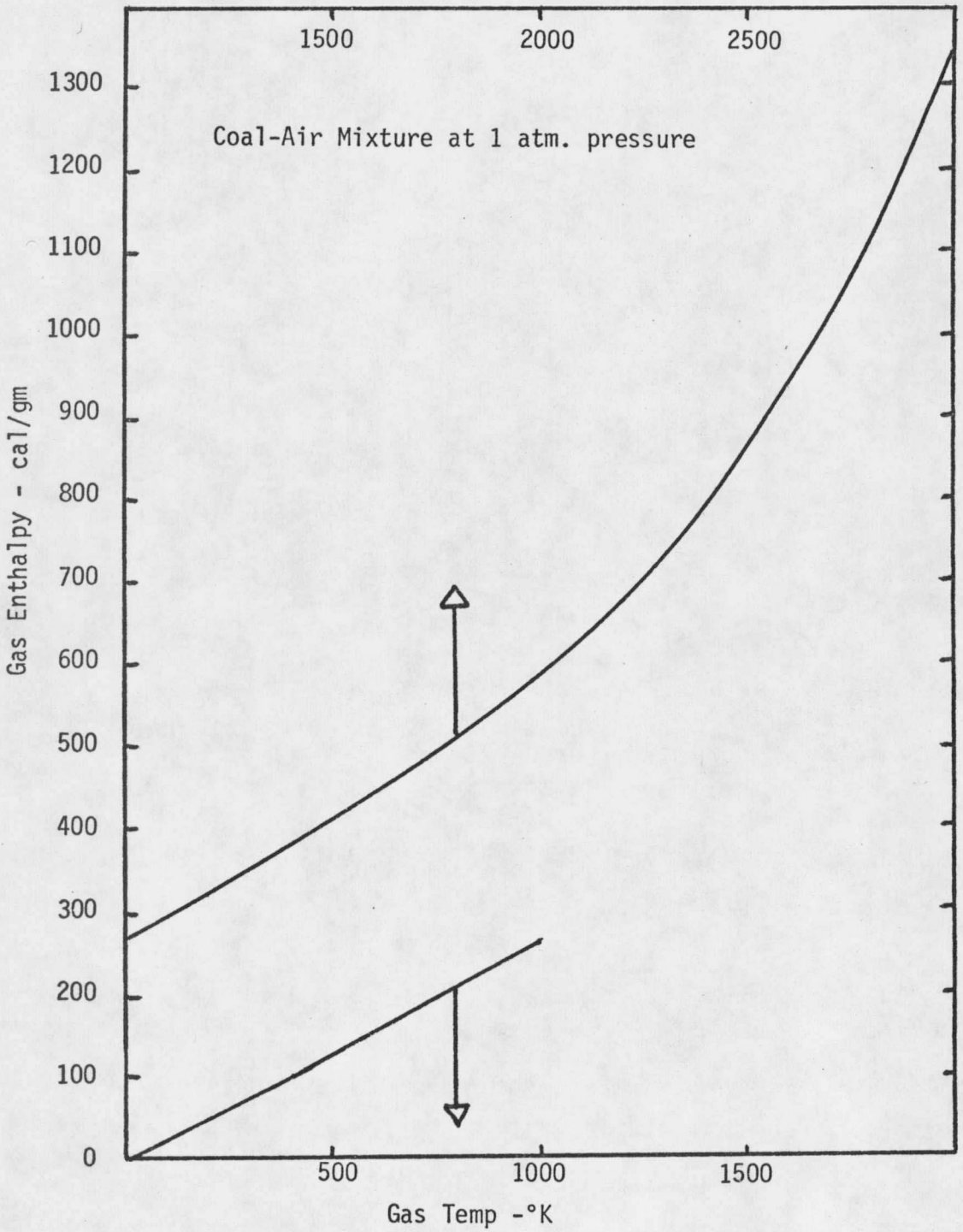

FIGURE 8. ENTHALPY OF MHD COAL EXHAUST GAS vs. TEMPERATURE

APPENDIX B: GENERAL DESIGN BALANCES

1. Composition of Montana Sub-bituminous Coal (6)

Proximate Analysis (as received)	Weight Percent
Moisture	24.3
Volatile Matter	28.6
Fixed Carbon	39.6
Ash	7.5
	100.0

Ultimate Analysis (as received)	
Ash	7.5
Sulfur	0.8
Hydrogen	6.1
Carbon	52.2
Nitrogen	0.8
Oxygen	32.6
	100.0

Higher Heating Value 8944 BTU/lb_m

2. Air Input to 400 MW (Thermal) MHD Combustor

$$\text{Heat Input} = \frac{400 \times 10^6 \text{ Watt}}{1} \times \frac{3.414 \text{ BTU}}{\text{hr watt}} = 1.3656 \times 10^9 \text{ BTU/hr}$$

$$\text{Coal Rate} = 1.3656 \times 10^9 \text{ BTU/hr} \times \frac{lb_m}{8944 \text{ BTU}} = 1.527 \times 10^5 \frac{lb_m}{hr}$$

Formula for Moisture and Ash-Free Coal:

$$CH_{.8}O_{.08}N_{.02}S_{.008}$$

Combustion Reaction:

$$CH_{.8}O_{.08}N_{.02}S_{.008} + 1.178O_2 \rightarrow CO_2 + .4\ H_2O + .02NO + .008SO_2$$

Assume molecular weight of coal = 14.62 (moisture and ash-free)

Air requirement for coal combustion:

$$\frac{1.178 \text{ mole } O_2}{\text{mole coal}} \times \frac{\text{mole coal}}{14.62 \text{ lb Coal}} \times \frac{32 \text{ lb } O_2}{\text{mole } O_2} \times \frac{100 \text{ lb Air}}{21 \text{ lb } O_2}$$

$$= \frac{12.28 \text{ lb Air}}{\text{lb coal (moisture-ash free)}}$$

The moisture and ash-free coal rate is:

$$(1.527 \times 10^5)(.682) = 1.041 \times 10^5 \text{ lb/hr}$$

Thus, the combustion air rate is:

$$\text{Air Rate} = \frac{1.041 \times 10^5 \text{ lb coal}}{\text{hr}} \times \frac{12.28 \text{ lb air}}{\text{lb coal}}$$

$$= 1.279 \times 10^6 \text{ lb air/hr}$$

3. Heat Transfer Rate to Air in Preheater

$$q_{air} = W_{air} \int_{1700°F}^{3100°F} C_{p_{air}}\, dT$$

$$= \frac{1.279 \times 10^6 \text{ lb air}}{\text{hr}} \times \frac{403.04 \text{ BTU}}{\text{lb}} = 5.155 \times 10^8 \text{ BTU/hr}$$

APPENDIX C: MODEL DEVELOPMENT OF FALLING-PARTICLE AIR PREHEATER

1. Particle Size Distribution

0.038 in. Blowout		0.042 in. Blowout	
Diameter, in.	No. Fraction	Diameter, in.	No. Fraction
0.05	0.011	0.05	0.0182
0.046	0.128	0.046	0.1033
0.044	0.256	0.045	0.2067
0.042	0.256	0.044	0.1550
0.040	0.193	0.0435	0.1034
0.039	0.105	0.043	0.1550
0.0375	0.051	0.042	0.2584

2. Terminal Velocity and Chamber Diameter Calculation

Terminal velocity is calculated using the general equation for spherical particles developed in McCabe and Smith, Unit Operations of Chemical Engineering, Second Edition, pp. 164-169:

$$U_T = \left(\frac{4}{3}\ \frac{g\,\rho_s}{18.5}\right)^{5/7}\ \frac{D^{8/7}}{\rho^{2/7}\ \mu^{3/7}} \qquad (1)$$

Now, assuming that $U_A = U_T$ for the smallest particle at the highest temperature:

$$W_A = U_A \rho A \qquad (2)$$

$$A = W_A/U_{A\rho} = \pi D_i^{\,2}/4$$

$$\therefore\ D_i = \left(\frac{4}{\pi}\ \frac{Wg}{U_b\,\rho}\right)^{1/2} \qquad (3)$$

With all gas properties evaluated at the highest chamber temperature.

Air Chamber: (properties evaluated at T = 3560°R)

0.038 in. Blowout			0.042 in. Blowout		
U_T, ft/sec	U_A, ft/sec	Di, ft	U_T, ft/sec	U_A, ft/sec	Di, ft
18.34	18.34	11.84	20.88	20.88	11.1

As an initial estimate, no heat losses were assumed; thus

$$q_{air} = q_{gas} = 2.578 \times 10^8 \text{ BTU/hr}$$

Gas Chamber:

To obtain the gas mass flow rate (wg), the following expression was used:

$$q_{gas} = Wg \int_{2300°F}^{3500°F} Cp_G \, dT \qquad (4)$$

The 2300°F exit temperature of the gas is also an estimate, which will subsequently be refined. From this calculation,

$$W_g = 6.52 \times 10^5 \text{ lb/hr}$$

Now, in analogous fashion to the air chamber diameter calculations, the gas chamber diameter is calculated. (Gas properties are developed at T = 3500°F = 3960°R).

0.038 in. Blowout		0.042 in. Blowout	
U_T = Ug, ft/sec	Di, ft.	U_T = Ug, ft/sec	Di, ft.
13.30	15.1	15.14	14.2

Note: Since the maximum temperature of the gas chamber occurs at the bottom of the chamber, this is where the terminal velocity calculations were made. However, since velocities at the top of the column are desired (to be analogous to the air column data), the above velocities are a result of multiplying the bottom terminal velocities by the factor 2760°R/3960°R, assuming the Ideal Gas Law to hold in this temperature range.

3. Determination of Insulation Thickness

The general equation for heat transfer between the gas in the column and ambient air is:

$$q/A_o = U_o (T_g - T_\infty) \qquad (5)$$

where

T_g = gas temperature

T_∞ = ambient air temperature

U_o = overall heat transfer coefficient based on outside column area

q/A_o = heat flux

and

$$\frac{1}{U_o} = \frac{A_o}{A_i h_i} + \Sigma R_{wall} + \frac{1}{h_o} \qquad (6)$$

h_i = inner wall convective heat transfer coefficient

h_o = outer wall convective heat transfer coefficient

ΣR_{wall} = sum of conductive heat transfer resistances in wall

$$\Sigma R_{wall} = \frac{\Delta r_1 A_o}{k_1 A_{lm_1}} + \frac{\Delta r_2 A_o}{k_2 A_{lm_2}} + \frac{\Delta r_3 A_o}{k_3 A_{lm_3}} + \frac{\Delta r_4 A_o}{k_4 A_{lm_4}} \qquad (7)$$

Natural convection is assumed between the outer wall and air. The resistance to heat transfer of the steel structure on the outside of the insulation is assumed small relative to the insulation resistance, and is neglected. From Perry's (10), the correlation for the outer convective heat transfer coefficient is:

$$h_o = 0.18 \, (T_w - T_\infty)^{1/3} \qquad (8)$$

for $GrPr > 10^9$

Since T_w is unknown, T_w is needed as a function of T_g, the gas temperature:

From equation 6:

$$\frac{h_o}{U_o} = 1 + h_o \left(\Sigma R_w + \frac{A_o}{A_i h_i} \right) \qquad (9)$$

Now, since $q/A_o = h_o(T_w - T_\infty)$, this can be equated to equation 5:

$$(T_g - T_\infty) = \frac{h_o}{U_o} (T_w - T_\infty) \qquad (10)$$

Substituting equation 9 into equation 10 gives:

$$(T_g - T_\infty) = (1 + h_o(\Sigma R_w + \frac{A_o}{A_i h_i}))(T_w - T_\infty) \qquad (11)$$

Substitution of equation 8 into equation 11 gives:

$$(T_g - T_\infty) = (T_w - T_\infty) + .18\,(T_w - T_\infty)^{4/3}(\Sigma R_{wall} + \frac{A_o}{A_i h_i}) \qquad (12)$$

- or -

$$(T_g - T_\infty) = (T_w - T_\infty) + .18\,(T_w - T_\infty)^{4/3}(\Sigma R_{wall} + \frac{r_o}{r_i h_i}) \qquad (13)$$

where

$$\Sigma R_{wall} = r_o\left[\frac{\ln(\frac{r_1}{r_i})}{k_1} + \frac{\ln(\frac{r_2}{r_1})}{k_2} + \frac{\ln(\frac{r_3}{r_2})}{k_3} + \frac{\ln(\frac{r_o}{r_3})}{k_4}\right]$$

NOTE: In this design h_i is assumed to be 10 BTU/hrft^2°F.

4. Wall Heat Loss Determination

Initially, T_w is found for various values of T_g using equation 12 in Appendix C-3. Then $(q/A)_{loss}$ is found for these values using equation 5 in Appendix C-3. A curve is then fit to the data, resulting in the following equation:

$$(q/A)_{loss} = -44.9 + .0612\,T_g, \quad T_g = °R \qquad (14)$$

$$(q/A)_{loss} = \text{BTU/hrft}^2$$

5. Overall Heat Loss Determination

Using equation 14, an average heat loss is found for each chamber:

$$(q/A)_{L_{air}} = 116.3 \frac{BTU}{hrft^2} \qquad (q/A)_{L_{gas}} = 146.3 \frac{BTU}{hrft^2}$$

Now, assuming that $L_{gas} = 20$ ft and $L_{air} = 30$ ft and $D_{o_{gas}} = (14.2 + 7.0) = 21.2$ ft , $D_{o_{air}} = (11.1 + 7.0) = 18.1$ ft

$$q_L = (q/A)_L \, \pi(D_o)(L) \tag{15}$$

$\therefore q_{L_{gas}} = (146.3)(\pi)(21.2)(20) = 1.95 \times 10^5$ BTU/hr

$q_{L_{air}} = (116.3)(\pi)(18.1)(30) = 1.98 \times 10^5$ BTU/hr

$q_{L_{recycle}} = \frac{1}{2} (3.933 \times 10^5) = 1.97 \times 10^5$ BTU/hr

The overall heat loss, then is:

$$q_{L_{overall}} = (1.95 + 1.98 + 1.97) \times 10^5 = 5.9 \times 10^5 \text{ BTU/hr}$$

An overall energy balance gives:

$$q_{air} + q_{loss} \simeq q_{gas} = -W_g \int_{T_o}^{3960°R} Cp_g dT \tag{16}$$

T_o is the only unknown in this equation:

$$T_o = 2790°R = 2330°F$$

which agrees closely with the original estimate for the gas exit temperature of 2300°F. An energy balance between the solids and the air in the air chamber gives:

$$q_{solids} = q_{air} + q_{L_{air}} \qquad (17)$$

$$W_s \int_{2475°R}^{3760°R} C_{p_s} dT = (2.578 \times 10^8 + 1.98 \times 10^5) \text{ BTU/hr}$$

which gives $W_s = 6.54 \times 10^5$ lb/hr

6. Development of Design Equations

Equations will be developed for the air column; thus $T_g > T_s$ at any point in the column. Also, it is assumed that X (vertical position) equals 0 at the top of each column.

1) Energy Balance Between Particles and Air across Differential Time Element:

$$W_s C_{p_s} T_s \Big|_{\theta+\Delta\theta} - W_s C_{p_s} T_s \Big|_{\theta} = -hA_s(T_s - T_g) \qquad (18)$$

where A_s = total surface area of particles falling in time element $\Delta\theta$

$$A_s = (\text{Particle Vol. in } \Delta\theta)\left(\frac{\text{Surface Area}}{\text{Volume}}\right)_{\text{particle}}$$

$$= \left(\frac{W_s}{\rho_s}\Delta\theta\right)\left(\frac{\pi d_p^2}{\frac{\pi d_p^3}{6}}\right) = \frac{6W_s}{d_p\rho_s}\Delta\theta \qquad (19)$$

$$W_s C_{p_s} \frac{dTs}{d\theta} = 6\,\frac{hWs}{d_p\rho_s}(T_g - T_s)$$

$$\frac{dT_s}{d\theta} = \frac{6h}{d_p \rho_s Cp_s} (T_g - T_s) \tag{20}$$

Note: In all design equations, the independent variable is to be x-vertical distance. Thus, to transform the above equation,

$$\frac{dT_s}{dx} = \left(\frac{dT_s}{d\theta}\right)\left(\frac{d\theta}{dx}\right) = \frac{dT_s}{d\theta} \left(\frac{1}{V}\right) \tag{21}$$

$$\therefore \frac{dT_s}{dx} = \frac{6h}{d_p \rho_s Cp_s V} (T_g - T_s)$$

(This is program statement 93.00)

2) X-Direction Momentum Balance on One Particle:

$$\Sigma (\text{x-direction forces}) = \frac{ma_x}{g_c} \tag{22}$$

$$\frac{ma_x}{g_c} = \frac{mg}{g_c} - F_d$$

$$ma_x = g - F_d g_c$$

$$\frac{\pi d_p^3}{6} \rho_s \frac{dV}{d\theta} = \frac{\pi d_p^3}{6} \rho_s g - F_d g_c \tag{23}$$

where F_d is the drag force on the particle (9) and A_c is the particle cross-sectional area.

From (9), $F_d = \dfrac{C_D \rho_g (V+U)^2 A_c}{2 g_c}$

$$\therefore \frac{\pi d_p^3}{6} \rho_s \frac{dV}{d\theta} = \frac{\pi d_p^3}{6} \rho_s g - C_D \frac{\rho_g (V+U)^2}{2g_c} \cdot \frac{\pi d_p^2 g_c}{4} \quad (24)$$

$$\frac{dV}{d\theta} = g - \frac{3C_D \rho_g}{4 d_p \rho_s} (V+U)^2$$

Again, since the independent variable x is desired,

$$\frac{dV}{dx} = \frac{dV}{d\theta} \cdot \frac{d\theta}{dx} = \frac{dV}{d\theta} \cdot \frac{1}{V} \quad (25)$$

$$\therefore \frac{dV}{dx} = \frac{g}{V} - \frac{3C_D \rho_g (V+U)^2}{4 d_p \rho_s V} \quad \text{(program statement 95.00)} \quad (26)$$

This equation, when integrated, gives V as a function of x. It can be integrated again to give θ as a function of x:

$$\frac{d\theta}{dx} = \frac{1}{V} \quad \text{(program statement 96.00)} \quad (27)$$

3) Overall Energy Balance Across Differential Column Element ΔX:

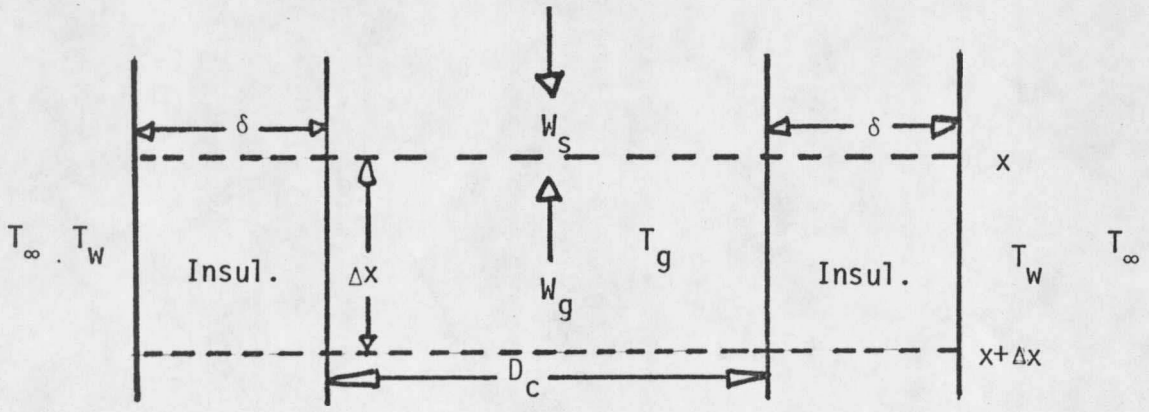

$$[W_g Cp_g (T_g - T_{ref})|_{x+\Delta x} - W_g Cp_g (T_g - T_{ref})|_x]$$

$$- (q/A)_L \pi (D_c + 2\delta) \Delta x = -h_s (\text{Particle Surface Area in } \Delta x)(T_s - T_g) \quad (28)$$

where particle surface area in Δx =

$$\frac{Ws}{\rho_s} \Delta\theta \left(\frac{S.A.}{Vol.}\right)_{particle} = \frac{Ws}{\rho_s} \frac{\Delta x}{\frac{dx}{d\theta}} \left(\frac{\pi d_p^2}{\frac{\pi d_p^3}{6}}\right)$$

$$= \frac{6 Ws \Delta x}{\rho_s d_p} \frac{d\theta}{dx}$$

Thus, equation 28 becomes

$$\frac{dT_g}{dx} = \frac{(q/A)_L \pi (D_c + 2\delta)}{W_g Cp_g} - h_s \frac{6 W_s}{\rho_s d_p} \frac{d\theta}{dx} (T_s - T_g) \quad (29)$$

Now, solving equation 20 for $(T_s - T_g)$ and substituting this value into equation 29:

$$\frac{dT_g}{dx} = \frac{(q/A)_L \pi (D_c + 2\delta)}{W_g Cp_g} + \frac{W_s Cp_s}{W_g Cp_g} \frac{dT_s}{dx} \quad (30)$$

The first term on the right in the above equation is labeled XX in program statement 104.00. The second term is labeled YY (7) in program statement 99.00. Their sum and the resulting differential equation are program statement 105.00.

7. Definitions of Program Variables and Program Listing

(listed in order of appearance in program with statement number)

Statement No.		
	M:	size iteration for particles (M = 1-7)
4.00	TEMPG:	gas temperature at top of chamber,°R
5.00	TP:	particle temperature at top of chamber,°R
6.00,7.00	A,B:	constants in gas viscosity equation
8.00,9.00	C,D:	constants in gas thermal conductivity equation
10.00	F:	constant in gas density equation
11.00	P:	chamber pressure, atm
12.00	UG:	gas velcoity at top of chamber, ft/sec
13.00,14.00 15.00	AB,BB,BC:	constants in gas heat capacity equation
16.00	DS:	overall chamber diameter, including insulation, ft
17.00	WG:	gas mass flow rate, lb/hr
18.00	W:	particle mass flow rate, lb/hr
20.00-26.00	DP(M):	diameter of particle 'M', ft
31.00-37.00	FR(M):	number fraction of total particles of size 'M'
43.00	IO:	integration order
44.00	VP:	initial particle velocity
45.00-46.00	AA,AG:	constants in heat loss equation
48.00	V(M):	velocity of particle of size 'M', ft/sec
49.00	T(M):	time, seconds

50.00 TS(M): temperature of particles of size 'M',°R

55.00 WS(M): $$\frac{W \cdot FR(M) \frac{\pi D(M)^3}{6} \rho_s}{\sum_{M=1}^{7} FR(M) \frac{\pi D(M)^3}{6} \rho_s} = \frac{W \cdot FR(M) D(M)^3}{WB(7)}$$

= mass flow rate of particles of size'M', lb/hr

79.00 TG: gas temperature,°R

80.00 DENG: gas density, lb/ft^3

81.00 DENS: particle density, 232 lb/ft^3

82.00 VIS: gas viscosity, $lb_m/ftsec$

83.00 KG: gas thermal conductivity, BTU/hrft°F

84.00 U: gas velocity at temperature TG, ft/sec

85.00 G: (Viscosity/density)(3600), ft^2/hr

86.00 PR: (gas heat capacity)(visocity)/(conductivity), dimensionless

88.00 TH: particle thermal conductivity, BTU/hrft°F

90.00 R(M): particle Reynolds number of particle size, 'M', dimensionless

91.00 H: particle surface convective heat transfer coefficient BTU/$hrft^2$°F, from: $Nu = 0.2Re^{.7}Pr^{1/3}$ (Reference 13)

92.00 Z: particle heat capacity, BTU/lb_m°F

94.00-94.21 CD: drag coefficient, dimensionless (three different expressions for drag coefficient are given for three different ranges of Reynolds number)

97.00 YZ: gas heat capacity, BTU/lb_m°F

98.00 S(M): stress on particle of size 'M', psi

99.00	YY(M):	heat transfer rate between particles of size 'M' and gas, BTU/hr
101.00	TEMPP(7):	weighted average particle temperature for all particles
103.00	Q:	q/A (heat loss to walls per unit outside area), $BTU/hrft^2$
104.00	XX:	total heat loss from chamber wall, BTU/hr

NOTE: For information on general Fortran format and subroutines, see reference (18).

```
 1.000        NAME LIST
 2.000       DIMENSIØN TS(7),V(7),WS(7),R(7),DTS(7),TEMPP(0:7),
 3.000      1DV(7),T(7),DT(7),DP(7),S(7),FR(7),YY(0:7),WB(0:7)
 4.000       TEMPG=3560.
 4.500       YY(0)=0.
 5.000       TP=3760.
 6.000       A=.000000607
 7.000       B=.513
 8.000       C=.0004736
 9.000       D=.583
10.000       F=39.12
11.000       P=8.
12.000       UG=20.88
13.000       AB=.2261
14.000       BB=.000028295
15.000       BC=-.000000002286
16.000       DS=18.1
17.000       WG=6.395E5
18.000       W=6.54E5
19.000        REAL KG
20.000       DP(1)=.05/12
21.000       DP(2)=.046/12
22.000       DP(3)=.045/12
23.000       DP(4)=.044/12
24.000       DP(5)=.0435/12
25.000       DP(6)=.043/12
26.000       DP(7)=.042/12
31.000       FR(1)=.0182
32.000       FR(2)=.1033
33.000       FR(3)=.2067
34.000       FR(4)=.1550
35.000       FR(5)=.1034
36.000       FR(6)=.1550
37.000       FR(7)=.2584
42.000       INPUT DX,X,PI,PF
```

```
43.000          I0=2
44.000          VP=.1
45.000         AA=-44.9
46.000         AG=.0612
47.000         D0 149 M=1,7
48.000          V(M)=VP
49.000          T(M)=0.
50.000          TS(M)=TP
51.000         WB(0)=0.
52.000         WB(M)=WB(M-1)+FR(M)*(DP(M)**3)
53.000 149      CONTINUE
54.000         D0 12 M=1,7
55.000         WS(M)=FR(M)*(DP(M)**3)*W/WB(7)
56.000 12       CONTINUE
57.000 1        INPUT
58.000          WRITE (108,900)
59.000 900      FORMAT('POSITION',4X,'TS(1)',7X,'TS(2)',7X,
60.000       1'TS(3)',7X,'TS(4)',7X,'TS(5)')
61.000          WRITE (108,901)
62.000 901      FORMAT('TS(6)',7X,'TS(7)',7X,'TS(8)',7X,'TS(9)',7X,
63.000       1'TS(10)',6X,'TS(11)')
64.000          WRITE (108,902)
65.000 902      FORMAT('GAS TEMP',4X,'V(1)',8X,'V(2)',8X,'V(3)',8X,
66.000       1'V(4)',8X,'V(5)')
67.000          WRITE (108,903)
68.000 903      FORMAT('V(6)',8X,'V(7)',8X,'V(8)',8X,'V(9)',8X,
69.000       1'V(10)',7X,'V(11)')
70.000          WRITE (108,904)
*
```

```
71.000 904     FORMAT('STRESS(1)',3X,'STRESS(2)',3X,'STRESS(3)',3X,
72.000        1'STRESS(4)',3X,'STRESS(5)',3X,'STRESS(6)')
73.000          WRITE (108,905)
74.000 905     FORMAT('STRESS(7)',3X,'STRESS(8)',3X,'STRESS(9)',3X,
75.000        1'STRESS(10)',2X,'STRESS(11)',2X,'PRANDL NUM')
76.000          WRITE (108,906)
77.000 906     FORMAT('MAX REY NUM',1X,'MIN REY NUM',1X,'PART TEMP',3X,

78.000        1'GAS VEL',5X,'MAX TIME',4X,'MIN TIME')
79.000          TG=TEMPG
80.000 20       DENG=F*(P/TG)
81.000         DENS=232.
82.000          VIS=A*(TG**B)
83.000          KG=C*(TG**D)
84.000          U=UG*(TG/TEMPG)
85.000          G=(A/C)*(TG**(B-D))*3600.
86.000          PR=G*(AB+BB*TG+BC*(TG**2))
87.000        DO 13 M=1,7
88.000          TH=2.91+(2.918E-6)*(TS(M)-2760.)**2
89.000        1-(1.5611E-12)*(TS(M)-2760.)**4
90.000          R(M)=DENG*(U+V(M))*DP(M)/VIS
91.000          H=KG*(.2*(R(M)**.7)*(PR**.334))/DP(M)
92.000          Z=.25667+.000016339*TS(M)
93.000          DTS(M)=.00167*H*(TG-TS(M))/(DENS*DP(M)*Z*V(M))
93.100          IF(R(M).LE.1.),GO TO 99
93.200           IF(R(M).GE.500.),GO TO 800
94.000          CD=18.5/(R(M)**.6)
94.100          GO TO 98
94.200 99       CD=24./R(M)
94.205          GO TO 98
94.210 800      CD=.44
94.300 98     XXX=0.
95.000          DV(M)=32.17/V(M)-.75*CD*((V(M)+U)**2)*DENG/(DENS*(DP(M))
```

```
*V(M))
   96.000          DT(M)=1./V(M)
   97.000          YZ=AB+BB*TG+BC*(TG**2)
   98.000          S(M)=34.6*H*DP(M)*(TS(M)-TG)/TH
   99.000          YY(M)=YY(M-1)+DTS(M)*WS(M)*Z/(WG*YZ)
  100.000          TEMPP(0)=0.
  101.000          TEMPP(M)=TEMPP(M-1)+WS(M)*TS(M)/W
  102.000  13      CONTINUE
  103.000         Q=AA+AG*(TG+TEMPP(7))/2.
  104.000          XX=3.14*Q*DS/(WG*YZ)
  105.000         DTG=XX+YY(7)
  106.000          CALL PRNTF(PI,PF,NF,X,TS(1),TS(2),TS(3),TS(4),TS(5))
  107.000         CALL PRNTR(0,TS(6),TS(7),0.,0.,0.,0.)
  108.000          CALL PRNTR(0,TG,V(1),V(2),V(3),V(4),V(5))
  109.000         CALL PRNTR(0,V(6),V(7),0.,0.,0.,0.)
  110.000          CALL PRNTR(0,S(1),S(2),S(3),S(4),S(5),S(6))
  111.000         CALL PRNTR(0,S(7),0.,0.,DS,0.,0.)
  112.000         CALL PRNTR(1,R(1),R(7),TEMPP(7),J,T(7),T(1))
  113.000          GO TO (100,1),NF
  114.000  100     CALL INTI(X,DX,IO)
  115.000         DO 200 M=1,7
  116.000          CALL INT(TS(M),DTS(M))
  117.000          CALL INT(V(M),DV(M))
  118.000          CALL INT(T(M),DT(M))
  119.000  200     CONTINUE
  120.000          CALL INT(TG,DTG)
  121.000          GO TO 20
  122.000          END
*
```

```
*
!FORT4 CDJ
 EXT. FORTRAN IV, VERSION FØØ
OPTIONS >NS

!RUN $;:LIB.234
      LINKING $
      LINKING  :LIB
'P1' ASSOCIATED.
      LINKING  SYSTEM LIB
?.Ø1,Ø.,2.,4Ø.
?*
POSITION     TS(1)        TS(2)        TS(3)        TS(4)        TS(5)
TS(6)        TS(7)        TS(8)        TS(9)        TS(10)       TS(11)
GAS TEMP     V(1)         V(2)         V(3)         V(4)         V(5)
V(6)         V(7)         V(8)         V(9)         V(10)        V(11)
STRESS(1)    STRESS(2)    STRESS(3)    STRESS(4)    STRESS(5)    STRESS(6)
STRESS(7)    STRESS(8)    STRESS(9)    STRESS(10)   STRESS(11)   PRANDL NUM
MAX REY NUM  MIN REY NUM  PART TEMP    GAS VEL      MAX TIME     MIN TIME
   .00000       3760.0       3760.0       3760.0       3760.0       3760.0
   3760.0       3760.0        .00000       .00000       .00000       .00000
   3560.0        .10000       .10000       .10000       .10000       .10000
    .10000       .10000       .00000       .00000       .00000       .00000
   655.25       618.10       608.66       599.16       594.38       589.59
   579.96        .00000       .00000       18.100        .00000       .00000
   190.79       160.26       3760.0       20.880        .00000       .00000

   1.9999       3644.0       3602.0       3584.6       3561.4       3546.7
   3529.0       3480.3        .00000       .00000       .00000       .00000
   3329.9       4.3615       3.1250       2.7525       2.3494       2.1359
   1.9146       1.4514        .00000       .00000       .00000       .00000
   1169.7       930.46       852.06       758.74       703.78       640.93
   479.09        .00000       .00000       18.100        .00000       .00000
   240.38       177.33       3549.0       19.530       2.4810        .78819
```

3.9998	3561.7	3498.2	3474.1	3444.2	3426.6
3406.9	3360.2	.00000	.00000	.00000	.00000
3204.8	5.5544	3.9784	3.5330	3.0687	2.8304
2.5887	2.0975	.00000	.00000	.00000	.00000
1402.5	1064.6	959.38	839.78	772.96	700.38
535.00	.00000	.00000	18.100	.00000	.00000
259.62	187.12	3434.2	18.797	3.6124	1.1891
5.9996	3483.6	3404.9	3377.1	3344.6	3326.3
3306.8	3264.0	.00000	.00000	.00000	.00000
3099.0	6.3494	4.5980	4.1227	3.6361	3.3895
3.1411	2.6406	.00000	.00000	.00000	.00000
1592.1	1180.1	1057.0	921.82	848.92	772.27
608.64	.00000	.00000	18.100	.00000	.00000
275.10	196.14	3337.1	18.176	4.4581	1.5244
7.9995	3407.7	3318.0	3288.3	3254.9	3236.9
3218.0	3178.6	.00000	.00000	.00000	.00000
3003.5	6.9750	5.1231	4.6334	4.1366	3.8862
3.6348	3.1298	.00000	.00000	.00000	.00000
1766.3	1291.7	1154.5	1007.6	930.39	850.96
687.92	.00000	.00000	18.100	.00000	.00000
289.21	204.95	3249.5	17.616	5.1519	1.8242
9.9993	3333.5	3236.0	3205.3	3171.9	3154.3
3136.3	3099.7	.00000	.00000	.00000	.00000
2914.7	7.5095	5.5966	5.0991	4.5970	4.3446
4.0916	3.5840	.00000	.00000	.00000	.00000
1935.0	1402.7	1252.9	1095.8	1014.8	932.79
768.61	.00000	.00000	18.100	.00000	.00000
302.81	213.78	3168.0	17.095	5.7480	2.1000

11.999	3260.7	3157.6	3126.6	3093.6	3076.6
3059.4	3025.1	.00000	.00000	.00000	.00000
2830.7	7.9885	6.0369	5.5349	5.0297	4.7762
4.5223	4.0131	.00000	.00000	.00000	.00000
2102.0	1512.9	1351.1	1184.1	1099.5	1014.7
847.99	.00000	.00000	18.100	.00000	.00000
316.34	222.77	3090.9	16.602	6.2747	2.3578
13.999	3189.2	3082.3	3051.3	3019.0	3002.6
2986.1	2953.6	.00000	.00000	.00000	.00000
2750.2	8.4303	6.4536	5.9489	5.4419	5.1877
4.9332	4.4232	.00000	.00000	.00000	.00000
2267.4	1620.4	1446.5	1270.0	1181.6	1094.0
923.76	.00000	.00000	18.100	.00000	.00000
330.05	232.01	3017.0	16.130	6.7489	2.6011
15.999	3118.9	3009.4	2978.6	2947.1	2931.2
2915.4	2884.5	.00000	.00000	.00000	.00000
2672.4	8.8459	6.8525	6.3462	5.8381	5.5836
5.3287	4.8183	.00000	.00000	.00000	.00000
2429.3	1722.1	1536.4	1350.5	1258.5	1167.9
993.84	.00000	.00000	18.100	.00000	.00000
344.12	241.58	2945.7	15.674	7.1817	2.8324
17.998	3049.6	2938.5	2908.1	2877.4	2862.0
2846.8	2817.2	.00000	.00000	.00000	.00000
2596.8	9.2419	7.2375	6.7302	6.2216	5.9669
5.7119	5.2014	.00000	.00000	.00000	.00000
2584.5	1815.2	1617.9	1423.0	1327.7	1234.4
1056.4	.00000	.00000	18.100	.00000	.00000
358.69	251.56	2876.5	15.231	7.5808	3.0533

19.997	2981.3	2869.3	2839.4	2809.4	2794.5
2779.8	2751.2	.00000	.00000	.00000	.00000
2522.9	9.6230	7.6113	7.1035	6.5947	6.3399
6.0849	5.5746	.00000	.00000	.00000	.00000
2728.5	1896.4	1688.4	1485.5	1387.1	1291.4
1110.2	.00000	.00000	18.100	.00000	.00000
373.90	262.01	2808.8	14.797	7.9519	3.2651
21.996	2913.8	2801.5	2772.1	2742.8	2728.3
2714.1	2686.5	.00000	.00000	.00000	.00000
2450.4	9.9921	7.9759	7.4679	6.9591	6.7045
6.4496	5.9396	.00000	.00000	.00000	.00000
2856.9	1963.5	1746.0	1536.4	1435.6	1338.1
1154.4	.00000	.00000	18.100	.00000	.00000
389.87	273.02	2742.5	14.372	8.2991	3.4687
24.005	2846.8	2734.5	2705.6	2677.0	2662.9
2649.1	2622.3	.00000	.00000	.00000	.00000
2378.7	10.353	8.3346	7.8268	7.3182	7.0638
6.8091	6.2996	.00000	.00000	.00000	.00000
2965.7	2015.1	1789.9	1575.2	1472.8	1374.1
1189.1	.00000	.00000	18.100	.00000	.00000
406.81	284.72	2676.9	13.951	8.6274	3.6661
26.003	2780.6	2668.7	2640.4	2612.4	2598.7
2585.2	2559.1	.00000	.00000	.00000	.00000
2308.1	10.705	8.6852	8.1777	7.6696	7.4154
7.1611	6.6522	.00000	.00000	.00000	.00000
3050.8	2050.5	1819.7	1602.0	1498.7	1399.6
1214.5	.00000	.00000	18.100	.00000	.00000
424.68	297.09	2612.4	13.537	8.9361	3.8557

28.002	2715.0	2603.7	2575.9	2548.5	2535.1
2521.9	2496.5	.00000	.00000	.00000	.00000
2238.2	11.050	9.0306	8.5236	8.0161	7.7622
7.5082	7.0001	.00000	.00000	.00000	.00000
3110.8	2070.6	1836.7	1617.8	1514.6	1415.8
1231.9	.00000	.00000	18.100	.00000	.00000
443.72	310.29	2548.6	13.127	9.2289	4.0393
30.001	2649.9	2539.3	2511.9	2485.1	2472.0
2459.1	2434.2	.00000	.00000	.00000	.00000
2168.7	11.390	9.3716	8.8652	8.3584	8.1049
7.8514	7.3441	.00000	.00000	.00000	.00000
3145.9	2077.2	1842.5	1624.4	1522.1	1424.4
1242.8	.00000	.00000	18.100	.00000	.00000
464.10	324.42	2485.3	12.720	9.5075	4.2173
32.000	2585.0	2475.3	2448.4	2422.1	2409.2
2396.6	2372.2	.00000	.00000	.00000	.00000
2099.6	11.726	9.7089	9.2033	8.6974	8.4444
8.1913	7.6850	.00000	.00000	.00000	.00000
3157.6	2072.8	1839.5	1624.0	1523.2	1427.1
1248.8	.00000	.00000	18.100	.00000	.00000
486.01	339.63	2422.4	12.314	9.7735	4.3901

APPENDIX D: MODEL DEVELOPMENT OF CORED-BRICK AIR PREHEATER

Bricks are assumed isothermal. The geometric porosity of bricks with .25-inch diameter holes is 25%.

AIR PREHEATER WITH DIFFERENTIAL ELEMENT:

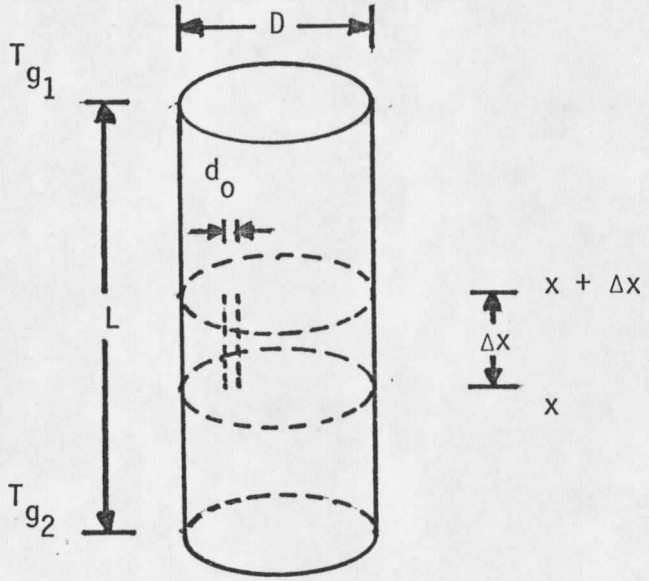

Energy Balance over Differential Element Δx:

heat input - heat output = heat transferred to/from bricks

$$W_g Cp_g T_g \big|_{x+\Delta x} - W_g\, p_g T_g \big|_x = 2h(P_x \Delta x)\Delta T \qquad (1)$$

where

$P_x = \pi d_o N_T$, N_T = number of holes in cross-section

$\Delta T = (T_{brick} - T_g)$

Note: The factor 2 accounts for the fact that, at any given time, gas will be flowing through <u>two</u> chambers.

$$W_g Cp_g \frac{dT_g}{dx} = 2hP_x \Delta T \tag{2}$$

$$W_g Cp_g dT_g = 2hP_x dx \Delta T \tag{3}$$

Defining $Nu = hd_o/k$ and integrating across the overall chamber length gives:

$$W_g Cp_g (T_{g_2} - T_{g_1}) = 2 \left(\frac{Nuk}{d_o}\right) P_x L \Delta T$$

or

$$L = \frac{W_g d_o}{Nu} \quad \frac{Cp_g}{k} \quad \frac{(T_{g_2} - T_{g_1})}{2\Delta T P_x} \tag{4}$$

Equation 4 can be written in terms of known dimenionless variables:

$$Re = \frac{U_b \rho d_o}{\mu} \qquad \text{where } U_b = \frac{W_g}{\rho A_h}$$

W_g = gas mass flow rate

A_h = total cross-sectional area of holes

$A_h = 2(\frac{1}{4})A_c$ for a geometric porosity of .25, for <u>two</u> chambers.

$$\therefore \quad U_b \rho = \frac{2W_g}{A_c}$$

A_c = cross-sectional area of one chamber

$$\therefore \quad Re = \frac{2W_g d_o}{\mu A_c} \tag{5}$$

$$Pr = \frac{Cp_g \mu}{k} \tag{6}$$

Substituting equations 5 and 6 into equation 4 gives:

$$L = \frac{RePrA_c(T_{g_2} - T_{g_1})}{Nu \ 4P_x \ \Delta T} \tag{7}$$

$$\frac{A_c}{P_x} = \frac{\text{Cross-sectional Area of holes}}{\text{Porosity}} \Big/ \text{Perimeter of holes}$$

$$= \frac{(N_T \frac{\pi d_o^2}{4})}{N_T \pi d_o} = d_o$$

And, St = Stanton Number = $\frac{Nu}{RePr}$

$$\therefore L = \frac{d_o(T_{g_2} - T_{g_1})}{St \ 4\Delta T} \tag{8}$$

The overall chamber length is calculated from equation 8. The chamber diameter is calculated from equation 5:

$$Re = \frac{2W_g d_o}{\mu A_c}$$

$$A_c = \frac{2W_g d_o}{\mu Re} = \frac{\pi D^2}{4}$$

$$\therefore \ D = \left[\frac{8W_g d_o}{\pi \mu Re}\right]^{\frac{1}{2}} \tag{9}$$

The length and diameter of the chamber are arrived at through a trial-and-error procedure. Reference (7) gives a graph of Re vs j_H, where

$$j_H = St \ Pr^{2/3} \tag{10}$$

This includes Reynolds numbers in both the laminar and turbulent-flow regions. Thus, for a given Reynolds number, the Stanton number can be found. Then L and D can be calculated, using equations 8 and 9, respectively. It is assumed that air is flowing through the chamber:

T_{g_2} = 3100°F

T_{g_1} = 1700°F

μ_{AV} = 3.3×10^{-5} lb_m/ftsec

Pr = .72

W_g = 1.279×10^6 lb/hr

ρ_{AV} = .13 lb/ft^3

d_o = 0.25 inches

According to the data of reference (17), a high Stanton number can be reached in the laminar flow region (Re < 2000). However, since diameter is inversely proportional to Re, the resulting design has a very large cross-sectional area, and a small column height. Thus, design parameters in the turbulent region are used. In this region, a maximum j_H of 0.0038 occurs at Re = 7000.

An average ΔT of 155°F is taken from established data for convective heat transfer from cored bricks to air (5). Incorporating this data into equations 8 and 9 gives:

At Re = 7000, St = .0047 from equation 10.

$L = 23.3$ ft

$D = 8.9$ ft

As a check, the chamber is sized assuming that hot gas is flowing through the chamber. Again, established data (5) gives an average ΔT between the hot gas and the cored bricks of 100°F. The following parameters are used:

$T_{g_2} = 3500°F$

$T_{g_1} = 2300°F$

$\mu_{AV} = 3.5 \times 10^{-5}$ $lb_m/ftsec$

$Pr = .72$

$\rho = .089$ lb_m/ft^3

$W_g = 1.304 \times 10^6$ lb_m/hr

$d_o = 0.25$ inches

Following the procedure outlined above, the following data are developed:

$L = 20.0$ ft $D = 8.7$ ft

Since the chamber dimensions calculated from air flow data are larger, they are considered conservative and are used in all subsequent calculations.

CHAMBER PRESSURE DROP

Pressure drop is calculated across the chamber height. The momentum equation for flow in a circular pipe gives (16):

$$\frac{-\Delta P}{\Delta L} = \frac{4\tau_w}{d_o} \tag{11}$$

where τ_w, the wall shear stress, can be defined in terms of the Fanning friction factor (9) as:

$$\tau_w = \frac{U_b^2 \rho f}{2g_c} \tag{12}$$

Substituting equation 12 into equation 11:

$$\frac{-\Delta P}{\Delta L} = \frac{2U_b^2 \rho f}{d_o g_c}$$

Now, since $Re = \frac{U_b \rho d_o}{\mu}$, we can write

$$\frac{-\Delta P}{\Delta L} = \frac{2f\mu^2 Re^2}{d_o^3 g_c \rho} \tag{13}$$

Or, over the overall chamber height L,

$$-\Delta P = \frac{2fL\mu^2 Re^2}{d_o^3 g_c \rho} \tag{14}$$

The Blasius equation (9) is used to define the Fanning friction factor in the turbulent flow region:

$$f = 0.079\ Re^{-\frac{1}{4}} \tag{15}$$

Thus, using equations 15 and 14 and employing the air flow data used previously, the chamber pressure drop is:

$$-\Delta P = 4.43 \text{ psi}$$

APPENDIX E: COST PREDICTION FOR FALLING-PARTICLE AIRE PREHEATER

1. Insulation Costs

Unit prices for refractory insulation material are presented in Appendix A-6. Initially, chamber volumes for each insulation type are calculated using

$$V = \frac{\pi}{4} (D_2^2 - D_1^2)L \qquad (1)$$

See Figure 5 for column insulation cross-section and designation of specific insulation types. Note: Hemispherical caps are assumed at each end of the column. Insulation costs for ends are doubled. The following data result:

(One Unit)		0.038 in. Blowout	0.042 in. Blowout
Insulation Volume (Ft^3)	Body	1.08×10^4	7500
	Ends	3200	2900
	Total	1.4×10^4	1.04×10^4
TOTAL COST		$\$ 1.73 \times 10^6$	$\$ 1.33 \times 10^6$

2. Steel Column Cost

To calculate the necessary steel thickness for the column, the following relation between pressure and tensile strength is used:

$$2\pi\sigma tL = 2\pi L\ pr \qquad (2)$$

where

r = column inside radius

t = steel thickness

p = column internal pressure

σ = steel tensile strength

L = column height

Thus, it follows that

$$t = \frac{pD}{2\sigma} \qquad (3)$$

where D is the column diameter (including insulation). A value of $\sigma = 1 \times 10^4$ psi is used for steel. Note: Again, hemispherical caps are assumed at each end of the column. Steel costs for ends are doubled. Using equation 3 to calculate the steel thickness gives the following data (a steel density of 490 lb_m/ft^3 is assumed):

(One Unit)		0.038 in. Blowout	0.042 in. Blowout
Steel	Body	4.37×10^5	2.93×10^5
Weight (lb_m)	Ends	1.6×10^5	1.4×10^5
	Total	5.97×10^5	4.33×10^5
TOTAL COST		$\$ 2.27 \times 10^6$	$\$ 1.72 \times 10^6$

3. Alumina Particle Cost

In predicting the mass of particles needed to initially charge the air preheater, it is assumed that a particle bed approximately 4 feet deep will lie above the top and middle distributor plates each, and at the chamber bottom. In addition, it is assumed that the particle mass in the pneumatic recycle system will about equal the mass of particles above one distributor plate. In predicting how much of the factory-supplied particle stock can be used in each blowout, it is assumed that 81% of the stock can be used to achieve a 0.038 in. blowout, and 54% of the stock can be used to achieve a 0.042 in. blowout. Using these figures and assuming a bed density of 135 lb_m/ft^3, the following particle masses are predicted (a particle cost of \$.25/lb_m is assumed):

0.038 in. Blowout: $M = 4.7 \times 10^5$ lb_m

$\text{Cost} = \$1.2 \times 10^5$

0.042 in. Blowout: $M = 6.1 \times 10^5$ lb_m

$\text{Cost} = \$1.5 \times 10^5$

These masses are of factory-delivered particle stock.

4. Miscellaneous Capital Costs

(a) Piping - a piping cost of \$1000/ft is assumed. In addition, it is assumed that 300 ft of piping is necessary for each unit. This

gives a piping cost of $\$3 \times 10^5$/unit.

(b) Valves - four valves are predicted per unit, at a cost of \$34,000/valve. This gives a valve cost of $\$1.36 \times 10^5$/unit.

(c) Instrumentation - it is assumed that instrumentation costs will be approximately $\$3 \times 10^5$ for the overall air preheat system. This figure is used for both blowout cases, and for the cored-brick system.

(d) Foundations and Structure - the overall capital cost for the foundations and structure of the unit is assumed to be 90% of the column steel cost.

5. Estimation of Annual Maintenance Costs

The major annual cost for the air preheater is particle replacement due to particle breakup and blowout. According to analysis done by W. E. Genetti, the turnover time during which the total particle bed must be replaced can be roughly estimated at 100 days. At a particle cost of $\$.15 \times 10^6$/unit, the annual particle replacement cost for two units is approximately $\$2.1 \times 10^6$.

APPENDIX F: COST PREDICTION FOR CORED-BRICK AIR PREHEATER

1. Insulation Costs

An insulation thickness of 3.5 feet is used for the cored-brick columns, the same as with the falling-particle column. See Figure 5 for insulation cross-section. Again, equation 1 in Appendix E-1 is used to calculate volumes for each insulation type.

Note: Hemispherical caps are assumed at each end of the column, and insulation costs for the ends are doubled.

(One Unit)	Insulation Volume, ft^3	Cost
Body	3168	$\$ 3.18 \times 10^5$
Ends	1763	3.44×10^5
TOTAL	8098	$\$6.62 \times 10^5$

2. Steel Column Cost

The relationship used to calculate the thickness of the steel column for the cored-brick air preheater is the same as that used in Appendix E-2 for the falling-particle air preheater. Knowing the column thickness, the total mass of steel necessary for the column can then be predicted.

Note: Again, hemispherical steel caps are assumed at each end of the column. Steel costs for the ends are doubled. A steel cost

of \$3/lb_m is assumed. ρ_{steel} = 490 lb_m/ft^3

(One Unit)	Steel Weight (lb_m)	Cost
Body	3×10^4	9×10^4
Ends	2.1×10^4	1.26×10^5
TOTAL	5.1×10^4	2.16×10^5

3. Cored Brick Costs

The cored brick heat transfer material used in this analysis is Norton AH299. The material has 0.25 inch cored holes giving it a 25% geometric cross-sectional porosity. It has an 18% material porosity and a purity of 99.5% alumina. The material cost is \$381/bulkft^3. It is assumed that the column is completely filled with cored brick.

$$\text{Volume} = \frac{\pi}{4} D^2 L = 1450 \text{ ft}^3$$

Cost of Cored Brick = $\$5.52 \times 10^5$

4. Miscellaneous Capital Costs

(a) Piping - a piping cost of \$1000/ft is assumed. A piping length of 1100 feet for the overall seven-unit air preheat complex is assumed. This gives a total piping cost of $\$1.1 \times 10^6$.

(b) Valves - it is assumed that four high-tmperature valves are needed for each column. Valve cost is \$34,000/valve. This gives a

valve cost of $\$1.36 \times 10^5$/unit.

(c) Instrumentation - as with the falling-particle air preheater system, it is assumed that overall instrumentation costs for the cored-brick system will be approximately $\$3 \times 10^5$.

(d) Foundations and Structure - the overall capital cost for foundation and structure for the cored-brick system is extrapolated from cost data supplied by W. E. Genetti for a direct-fired cored-brick air preheat system. This cost for the overall indirect-fired system is approximately $\$3 \times 10^6$.

5. Estimation of Annual Maintenance Costs

Annual costs for the cored-brick air preheater are mostly due to cored-brick replacement due to thermal shock and high-temperature corrosion. Estimated annual costs for a system of this capacity are found to be $\$1.4 \times 10^6$. The matrix lifetime is estimated at $\sim$ 1.7 years. This data is presented in reference (10).

APPENDIX G: DESIGN DATA FOR COAL CARBONIZATION SYSTEM

1. Mass and Energy Balances

All flow rates are labeled on Figured 6. From reference (10), the combustion air rate $\dot{A}'$ for the intermediate - BTU fuel gas is:

$$\dot{A}' = 12.47\ \dot{G} \tag{1}$$

Also from reference (10), coal carbonization yields the following:

$$2000\ lb_m\ Coal \rightarrow 1400\ lb_m\ coke + \sim 600\ lb\ fuel\ gas$$

Thus, using the nomenclature of Figure 6,

$$\dot{G} = \frac{600}{1400}\ \dot{K} \tag{2}$$

Now, to relate $\dot{A}$ and $\dot{G}$, an energy balance is taken across the air preheater (neglecting energy losses):

$$(\dot{G} + \dot{A}') \int_{2330°F}^{3500°F} Cp_{exhaust}\, dT = \dot{A} \int_{1700°F}^{3100°F} Cp_{air}\, dT \tag{3}$$

Using the heat capacity data from Appendix A in equation 3, and substituting in equations 1 and 2, gives:

$$\dot{K} = .1773\ \dot{A} \tag{4}$$

As an initial test, it is assumed that the fuel flow to the MHD combustor is pure coke, delivered at $T \simeq 1800°F$ from the coal carbonizer. From the requirement that the thermal input to the MHD duct be 400 MW, and noting that $\Delta H_{combustion} = 14{,}000\ BTU/lb_m$

and $C_p = .363$ BTU/lb_m°F for coke,

$$\dot{K}\Delta H_{comb} + \dot{K}C_p\ (1800°F - 77°F) = 1.366 \times 10^9 \qquad (5)$$

which yields $\dot{K} = 9.34 \times 10^4$ lb_m/hr. Now, from reference (10), the air requirement for combustion of coke is $\dot{A} = 11.2\dot{K}$. This gives an air flow rate of $\dot{A} = 1.046 \times 10^6$ lb_m/hr. Substituting this value into equation 4 gives the coke production rate necessary to produce enough fuel gas to heat this air flow rate:

$$\dot{K} = (.1773)(1.046 \times 10^6) = 1.855 \times 10^5\ lb_m/hr \qquad (6)$$

As can be seen, the coke flow rate from the carbonizer is nearly twice the coke flow rate to the MHD combustor.

APPENDIX H: DESIGN DATA FOR COAL GASIFICATION SYSTEM

1. Mass and Energy Balances

Flow rates are labeled on Figure 7. From reference (7), the conversion rate for the CO_2-acceptor gasification process is $\sim$ 60%. Then,

$$\dot{G} = .60\ \dot{D} \tag{1}$$

For the combustion of a high BTU gas, the air rate necessary is:

$$\dot{A}' = 17.24\dot{G} \tag{2}$$

Now, an energy balance across the air preheater yields (neglecting energy losses):

$$(\dot{G} + \dot{A}')\int_{2330°F}^{3400°F} Cp_{exhaust}\, dT = \dot{A}\int_{1700°F}^{3100°F} Cp_{air}\, dT \tag{3}$$

Note: a flame temperature of 3400°F is assumed for combustion of the gas (10). Also, the heat capacity of the combustion products is assumed to be close to that of the intermediate - BTU gas presented in Appendix A-3. Since ambient coal is being used in the MHD combustor, $\dot{A} = 1.279 \times 10^6$ lb_m/hr (see Appendix B-2). Substituting equation 2 into equation 3 and solving for $\dot{G}$ gives:

$$\dot{G} = 8.053 \times 10^4\ lb_m/hr \tag{4}$$

Using this value in equation 1 gives the coal input rate to the

gasifier:

$$\dot{D} = 1.34 \times 10^5 \text{ lb}_m/\text{hr} \qquad (5)$$

Since the coal flow rate to the MHD duct is 1.527×10^5 lb_m/hr (see Appendix B-2), the coal flow rate to the gasifier is ~47% of the total coal rate to the power generating complex.

2. Capital and Annual Cost Prediction

Reference (7) gives a capital cost of $\$103 \times 10^6$ for a CO_2 - acceptor gasification system with an output of 250×10^6 scf gas/day. Assuming a gas density of .051 lb_m/ft^3, an estimate of the capital cost of the gasification system for the air preheater is:

$$C = (103 \times 10^6)\left[\frac{8.053 \times 10^4}{1} \times \frac{(24)}{250\times10^6(.051)}\right]^{.7}$$

$$= \$27.5 \times 10^6$$

The annual operating cost of the 250×10^6 scf/day plant is given as $\$16 \times 10^6$. Thus, following the same procedure as above, the annual operating cost of the gasification system for the air preheater can be estimated as:

Annual operating cost = $\$4.3 \times 10^6$

BIBLIOGRAPHY

1. Rosa, Richard J., Notes, "EE 580 - MHD Power Conversion", Autumn 1975.

2. Rosa, R. J., Magnetohydrodynamic Energy Conversion, McGraw-Hill, Inc., 1968.

3. Shiendlin, A. E., and Jackson, W.D., "MHD Electrical Power Generation - An International Status Report", Ninth World Energy Conference, Detroit, 1974.

4. Hals, F. A., and Gannon, R. E., "Progress in Development of Auxiliary MHD Power Plant Components at Avco Everett Research Laboratory, Inc.", 74WA/Ener-6, published by the American Society of Mechanical Engineers.

5. Hals, F. A., and Gannon, R. E., "High Temperature Air Preheaters for Open Cycle MHD Energy Conversion Systems", published by Avco Everett Research Laboratory, Inc., Everett, Mass. 02149

6. Gannon, R. E., Hals, F. A., Stickler, D. B., "Methods of Coal Combustion and Processing in Open Cycle MHD Power Systems", MHD 117, published by Avco Everett Research Laboratory, Inc., Everett, Mass.02149.

7. Mudge, L. K., Schiefelbein, G. F., Li, C. T., Moore, R. H., "The Gasification of Coal", A Battelle Energy Program Report. July, 1974: Battelle Pacific Northwest Laboratories, Richland, Washington 99352.

8. Heywood, F. B., and Womack, G. F., Open Cycle MHD Power Generation, Pergamon Press, 1969.

9. Bennett, C. O., Meyers, J. E., Momentum Heat & Mass Transfer, 1962, McGraw-Hill Book Co., Inc., New York, N. Y.

10. Perry, J. H. (Ed.), Chemical Engineers' Handbook, Fourth Edition, 1963: McGraw-Hill, Inc., New York, N.Y.

11. Hals, F. A., written personal communication with the author.

12. Genetti, W. E., Mussulman, R. L., "Preliminary Design of a Direct-Fired, Falling Bed Air Preheater for an MHD Generator Test Facility".

13. Nakada, T., Nakamura, N., Narita, Y., Taira, T., "Studies of Falling Particles Regenerator", Proceedings of the Fifth International Conference on MHD Power Generation, April, 1971.

14. Smith, J. M., VanNess, H. C., Introduction to Chemical Engineering Thermodynamics, McGraw-Hill, 1959, Second Ed.

15. Kobe, K. A., and assoc., "Thermochemistry for the Petrochemical Industry", Petroleum Refiner, Jan. 1949, through Nov. 1954.

16. McCabe, W. L. and Smith, J. C.,"Unit Operations of Chemical Engineering, Second Ed., McGraw-Hill.

17. Knudsen, J. G. and Katz, D. L., Fluid Dynamics and Heat Transfer, McGraw-Hill, 1958.

18. Franks, Roger, G. E., Modeling and Simulation in Chemical Engineering, John Wiley & Sons, Inc. 1972.

Jensen, Chris D
Design of an indirect-fired falling-particle air preheater for MHD power generation

DATE	ISSUED TO
JAN 1 1985	Rick Sorrell 587-2513